REPORT 1201

PERFORMANCE AND BOUNDARY-LAYER DATA FROM 12° AND 23° CONICAL DIFFUSERS OF AREA RATIO 2.0 AT MACH NUMBERS UP TO CHOKING AND REYNOLDS NUMBERS UP TO 7.5×10^6 †

By B. H. Little, Jr. and Stafford W. Wilbur

SUMMARY

For each of two inlet-boundary-layer thicknesses, performance and boundary-layer characteristics have been determined for a 12°,10-inch-inlet-diameter diffuser, a 12°,21-inch-inlet-diameter diffuser, and a 23°,21-inch-inlet-diameter diffuser. The investigation covered an inlet Mach number range from about 0.10 to choking. The corresponding inlet Reynolds number, based on inlet diameter, varied from about 0.5 × 10^6 to 7.5 × 10^6.

Although small regions of separated flow existed in the 12° diffusers, the flow was relatively steady. In the 23° diffuser, the flow was badly separated and very unsteady. The addition of a uniformly rough layer of cork particles to the walls of the 23° diffuser eliminated the unsteadiness but did not improve the pressure recovery. Total-pressure losses increased and the static-pressure recovery decreased with increasing inlet-boundary-layer thickness for all three diffusers. Increasing flow rate (increasing Mach and Reynolds number) produced an adverse effect on performance which was very slight for the thinner inlet boundary layers in the 12° diffusers, but which became more severe with increasing inlet-boundary-layer thickness or increased diffuser angle.

INTRODUCTION

The performance of propulsion units which handle large quantities of air is strongly affected by the losses incurred in the associated duct systems. One of the most important components of these duct systems is the diffuser in which the performance depends upon the rate of geometric expansion, inlet Mach number and Reynolds number, and inlet-boundary-layer conditions. Although much diffuser research has been done, most of the data available (refs. 1 to 4) are at Mach numbers and Reynolds numbers too low to be of direct practical value in the design of aircraft-duct systems, are for improbable or often unknown inlet-boundary-layer conditions, and are taken from configurations with diffuser angles much nearer the optimum than can usually be obtained in practice.

The purpose of this report is to present performance and boundary-layer data for 12° and 23° conical diffusers of area ratio 2.0 under conditions representative of those encountered in flight. Data were obtained for two inlet-boundary-layer thicknesses in each diffuser. The 12° diffuser represents a borderline configuration between high- and low-performance diffusers and the 23° diffuser is typical of those often dictated by aircraft space limitations. Mach numbers are varied from about 0.10 to the Mach number at which the flow in the diffuser inlet choked, and Reynolds numbers range from about 0.5 to 7.5 × 10^6, based on inlet diameter. These data were originally obtained in three separate investigations in which the methods of presentation varied slightly. The data have been combined herein and some of the original nomenclature and reference points have been changed in the interest of clarity and uniformity.

SYMBOLS

p	static pressure
H	total pressure
r	radial distance from center line
r_d	duct radius
D	diameter
q_c	impact pressure $(H-p)$
ΔH	difference in mean total pressure at two survey stations
Δp	static-pressure rise through the diffuser
x	distance along longitudinal axis from reference station
y	perpendicular distance from diffuser wall
u	local velocity within boundary layer
U	local velocity at edge of boundary layer
δ	boundary-layer thickness at $\frac{u}{U}=0.95$
δ^*	boundary-layer displacement thickness for two-dimensional incompressible flow, $\int_0^{\delta'}\left(1-\frac{u}{U}\right)dy$
θ	boundary-layer momentum thickness for two-dimensional incompressible flow, $\int_0^{\delta'}\frac{u}{U}\left(1-\frac{u}{U}\right)dy$

† Supersedes recently declassified NACA RM's L9H10 by Martin R. Copp and Paul L. Klevatt, 1950, L9K10 by Jerome Persh, 1950, and L50C02a by B. H. Little, Jr. and Stafford W. Wilbur, 1950.

δ'	distance from surface beyond which the contribution to the integral of δ^* and θ is negligible
δ^*/θ	boundary-layer shape parameter for two-dimensional incompressible flow
m	mass flow
Δm	difference in measured mass flows at inlet and exit of diffuser
ρ	density
μ	coefficient of viscosity
M	Mach number
R	Reynolds number

Diffuser performance parameters:

$\Delta H/\bar{q}_{c_i}$	loss coefficient
$\Delta p/\Delta p_{ideal}$	diffuser effectiveness

Subscripts:

0	plenum-chamber stagnation conditions
i	diffuser-inlet station
e	diffuser-exit station
max	maximum
$ideal$	ideal condition

Bar over a symbol indicates a mean value.

APPARATUS

Line drawings of the diffusers used in this investigation are shown in figure 1. Two 12° diffusers were used—one with a 10-inch inlet diameter and the other with a 21-inch inlet diameter. A 23° diffuser with an inlet diameter of 21 inches was also used with the same inlet bell and approach ducting as the 12°, 21-inch diffuser. The ratio of exit area to inlet area for all three diffusers was 2.0. Inlet pipe lengths of 1 inlet diameter and 7 inlet diameters for the 12°,10-inch diffuser produced inlet boundary layers such that the ratios of inlet displacement thickness to inlet diameter $\frac{\delta^*_i}{D_i}$ were equal to 0.0039 and 0.0122; and inlet pipe lengths of ½ inlet diameter and 4½ inlet diameters for the 21-inch diffusers produced inlet boundary layers with $\frac{\delta^*_i}{D_i}$=0.0017 and 0.0095, respectively. The diffusers were connected to constant-area tailpipes about 2 diameters in length. The interior surfaces were made aerodynamically smooth.

The arrangement of static-pressure orifices was similar for all three diffusers. Six equally spaced static-pressure orifices were installed around the periphery at the inlet and exit and a row of orifices was placed along a generatrix of each diffuser. Similar static-pressure orifices lined the transition section joining the inlet length to the diffuser. All static-pressure orifices were connected to multitube manometers and pressures were recorded photographically. Total pressure and total temperature were measured in the plenum chamber upstream of the inlet bell.

The surveys from which mass flow and total-pressure loss were determined were made across the stream at the diffuser inlet and exit by electrically driven pitot-static tubes and by fixed rakes. Drawings of typical instrumentation are shown in figure 2. Similar instrumentation was used to make total-pressure surveys across the boundary layer at a number of other stations along the diffuser. The locations of all measuring stations are given in table I.

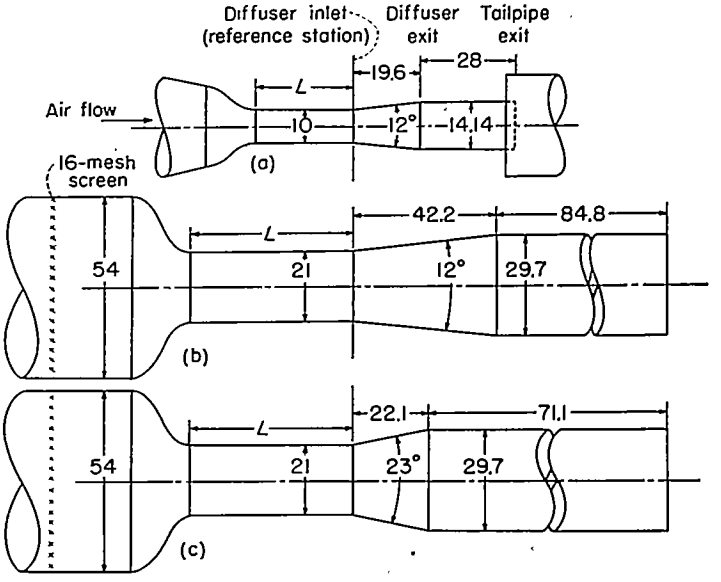

Diffuser	δ^*_i/D_i	L, in.
12°,10-inch	0.0039	9.0
	.0122	68.0
12°,21-inch	.0017	8.5
	.0095	97.5
23°,21-inch	.0017	8.5
	.0095	97.5

(a) 12° conical diffuser; inlet diameter, 10 inches.
(b) 12° conical diffuser; inlet diameter, 21 inches.
(c) 23° conical diffuser; inlet diameter, 21 inches.

FIGURE 1.—Arrangement of diffusers in duct systems.

COMPUTATIONAL METHODS AND ANALYSIS

Correlating parameter.—The requirement that the inlet duct and diffuser be free of all obstructions upstream of any station at which transverse pressure surveys were in progress made it impossible to survey at two stations simultaneously. In order to compare and combine measurements from different tests, the inlet-static-pressure ratio p_i/H_0 was used as a correlating parameter for the computation of the performance coefficients.

Inlet flow measurements.—Pressure surveys (from which the mass flow and mean total pressure were calculated) were made at the inlets (measuring position given in table I) of the three diffusers. Total pressure is presented only insofar as it is used in computing the change in total pressure through the diffuser. The mass-flow measurements were used to compute mean inlet Mach numbers and Reynolds numbers, which are plotted as functions of the correlating static-pressure ratios in figure 3. The mean inlet Reynolds number was obtained by using the mean value of flow density, the inlet diameter of the diffuser, and the viscosity based on stream static temperature; that is,

$$R_i=\frac{\overline{\rho_i u_i} D_i}{\mu}$$

Since the mean inlet mass flow decreased with increasing boundary-layer displacement thickness, separate curves of

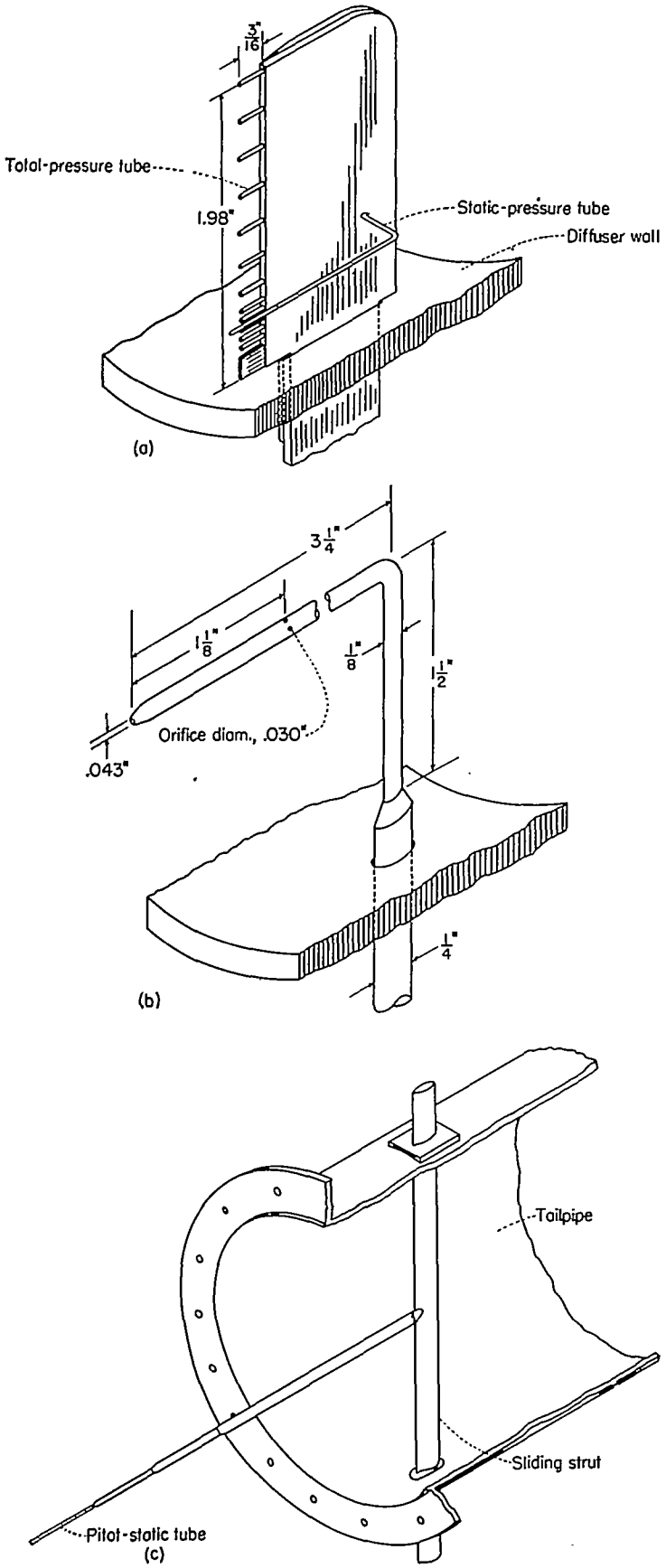

(a) Boundary-layer rake.
(b) Boundary-layer and mass-flow survey tube.
(c) Mass-flow survey tube.

FIGURE 2.—Typical instrumentation.

308555—56——65

$\overline{M}_i$ were obtained for the two boundary-layer conditions. The points of the Reynolds number curves varied so slightly with inlet boundary layer that only one curve, representing a mean fairing, is shown for each inlet diameter.

Although the inlet pressure ratios were adequate for correlation of various data for a given configuration, the mean inlet Mach number is a more satisfactory parameter for correlating data among the different configurations. Therefore, all performance data are plotted against mean inlet Mach number.

Boundary-layer parameters.—The ratio of local velocity in the boundary layer to the velocity at the edge of the boundary layer was obtained from the incompressible-flow relationship:

$$\frac{u}{U}=\sqrt{\frac{H-p}{(H-p)_{max}}}$$

The boundary-layer parameters (thickness δ, displacement thickness δ^*, momentum thickness θ, and shape factor δ^*/θ) were also obtained from the equations for incompressible flow with the added assumption that the boundary layer was two-dimensional. Since most of the data presented is in the range where local Mach numbers are less than 0.70 and since the incompressible equations have generally been used in the literature, this method of presentation was considered to be satisfactory. The error in δ^*/θ introduced by using the incompressible-flow relations is less than 5 percent except for the few cases where the local Mach number is greater than 0.70.

In some cases, the boundary-layer measurements were not extended to the point where $\frac{u}{U}=1.0$ because of survey-instrument limitations. For these cases the curves can be extrapolated without significant alteration of the results. At the highest flow rates in the 12° diffusers, total-pressure measurements indicated pressure deficiencies near the diffuser center line such as might be expected downstream of a region of supersonic flow. In these cases, $\frac{u}{U}$ was computed by use of the maximum measured value as U. In the graphical integration used to obtain δ^* and θ, velocity in the reversed-flow portion of the separated-flow profile was taken as zero. This procedure was considered adequate for purposes of determining trends in boundary-layer growth; however, the real significance of δ^* and θ in these cases is questionable and, consequently, no attempt was made to measure accurately reverse-flow velocities.

Performance parameters.—Two parameters, $\frac{\Delta H}{\overline{q}_{c_i}}$ and $\frac{\Delta p}{\Delta p_{ideal}}$, are used to present the performance data. The coefficient $\frac{\Delta H}{\overline{q}_{c_i}}$ (referred to as the loss coefficient herein) is the ratio of total-pressure loss through the diffuser to the mean inlet impact pressure. This parameter is convenient for use in evaluating the total loss in a duct-system component and is commonly used in the literature. It has the advantage of tending to remain constant with changes in flow rate as long as the basic flow pattern in a configuration does not

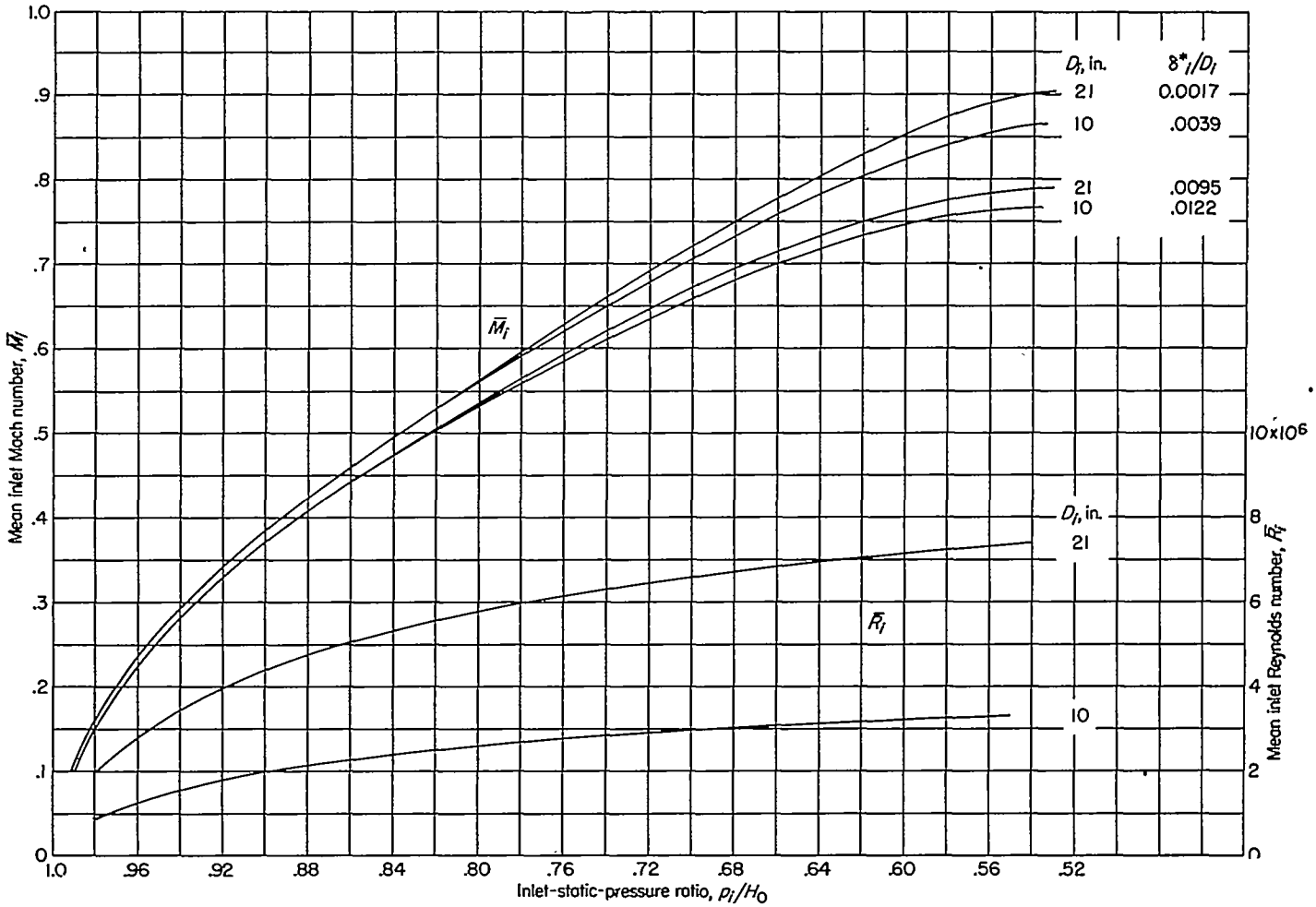

FIGURE 3.—Variation of mean inlet Mach and Reynolds numbers with inlet-static-pressure ratio.

change. The total-pressure loss is obtained from mass weighted averages of total pressure as follows:

$$\Delta H=\frac{\int_0^{r_d}\rho u\,(H_0-H_e)\,r\,dr}{\int_0^{r_d}\rho u r\,dr}-\frac{\int_0^{r_d}\rho u\,(H_0-H_i)\,r\,dr}{\int_0^{r_d}\rho u r\,dr}$$

where the values of ρ, u, H_i, H_e, and r are obtained for a large number of points in surveys at the inlets and exits of the diffusers and $\bar{q}_{c_i}$ is obtained from the formula

$$\bar{q}_{c_i}=H_0-\overline{(H_0-H_i)}-p_i$$

The value p_i is the inlet-wall static pressure for the 12° diffusers and the arithmetic mean of surveyed static pressures across the inlet station for the 23° diffuser.

The loss coefficient does not give any indication of the effectiveness of the diffuser in accomplishing the static-pressure rise and the corresponding velocity decrease for which the diffuser was intended. The parameter $\Delta p/\Delta p_{ideal}$ is used to measure that effect and is designated as diffuser effectiveness. The quantity Δp is the actual static-pressure rise from inlet to exit stations. This value is based on wall static pressures for the two 12° diffusers and on stream surveys for the 23° diffuser. The ideal pressure rise through the diffuser, Δp_{ideal}, was computed by use of one-dimensional isentropic relationships between static pressure and mass flow, the equation of continuity, and the assumption that the effective flow expansion is the same as the geometric expansion; that is, no boundary layer is assumed to be present. The ratio $\Delta p/\Delta p_{ideal}$ is lowered by anything which retards effective expansion of the flow such as boundary-layer growth or separation.

RESULTS AND DISCUSSION

The flow was steady in the 12°,21-inch diffuser and measurements were made with no difficulty. Slightly troublesome total-pressure fluctuations were observed in the 12°,10-inch diffuser. In the 23°,21-inch diffuser, total pressures fluctuated so violently at the diffuser exit that accurate surveys were not possible; however, at the tailpipe exit (2 diameters downstream of the diffuser exit) the flow was steady enough to permit surveys to be made. Since these flow instabilities in the 23° diffuser were caused by separation of the boundary-layer flow from the diffuser wall, roughening the surface was proposed in an attempt to eliminate or retard this separation. This proposal was based partly on the success of vortex generators in increasing turbulent mixing and thereby retarding separation and partly on the results presented in reference 5, which indicate

that roughening of an airfoil surface in the region of an adverse pressure gradient sufficiently changed the turbulent mixing process to produce the favorable result of reducing the profile drag. Small cork particles, approximately 0.10 inch in diameter, were cemented uniformly over essentially the entire surface (98 percent of the length) of the 23° diffuser. The roughness produced stable flow and permitted total-pressure measurements to be made at the diffuser exit. These and other roughened diffuser tests not pertinent to this investigation are reported in detail in reference 6.

In all tests, discrepancies were found to exist between mass-flow values measured at the inlet and exit stations of å configuration. Discrepancies of this type have been obtained in several diffuser investigations and an analysis of them based on certain hypotheses regarding the relation of impact-tube readings to turbulence is published in reference 7. These discrepancies are shown for all three diffusers in figure 4 where the ratio of measured difference in mass flow $\Delta m = m_e - m_i$ to measured inlet mass flow m_i is plotted against mean inlet Mach number. This ratio was positive (larger measured mass flow at the exit) for all configurations except for values of $\delta^*_i/D_i = 0.0017$ in the 12°,21-inch diffuser, for which the discrepancy was considered negligible except at high Mach numbers. The negative points for this case are within the limits of accuracy of these data. It seems logical that turbulence is, in part, responsible for these discrepancies because the effect of turbulent velocity fluctuations on a total-pressure tube is to produce a reading greater than the true value and also because the discrepancies were larger for the configurations with more unsteady flow. Owing to the nature of the inlet ducting arrangement it is assumed that the effect of turbulence on the inlet measurements is negligible and that the inlet-mass-flow measurements are correct. Therefore it is believed that the total-pressure-loss coefficients are low because turbulence generated in the diffuser produces erroneous readings of the mean exit total pressure. Similar errors in total-pressure measurements are presented and discussed in reference 7.

PERFORMANCE PARAMETERS

Total-pressure-loss coefficient.—The total-pressure-loss coefficient is plotted against mean inlet Mach number in figure 5 (a) for the two 12° diffusers and for the 23° diffuser with roughness. The same parameters are plotted in figure

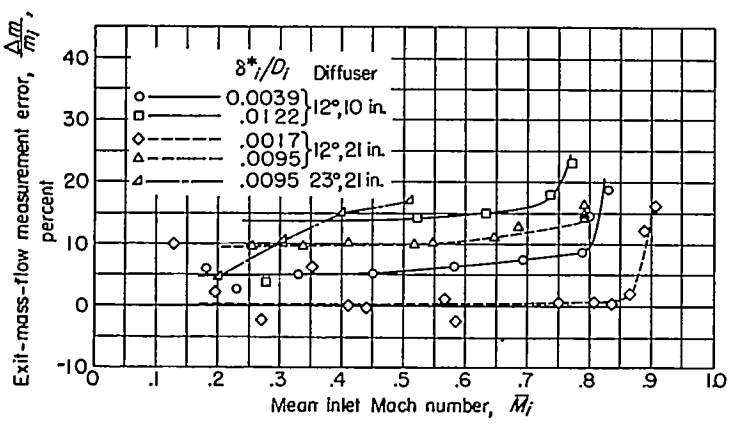

FIGURE 4.—Variation of the discrepancy between inlet- and exit-mass-flow measurements with mean inlet Mach number.

5 (b) for the 23° diffuser-tailpipe combination without roughness for the thinner inlet boundary layer, and both with and without roughness for the thicker inlet boundary layer ($\delta^*_i/D_i = 0.0095$). The latter pair of curves shows that, for the diffuser-tailpipe combination, roughening the walls had little effect on the values of loss coefficient. Therefore, it is believed that values of loss coefficient for the roughened diffuser closely approximate values for the smooth diffuser which were not measured; consequently, in figure 5 (a) the data for the roughened 23° diffuser are believed comparable with the data from the other diffusers. Although figure 5 (a) shows that in the 12° diffusers the measured values of loss coefficient are the same for $\delta^*_i/D_i = 0.0017$ and 0.0039, the systematic increase of $\Delta m/m$ with δ^*_i/D_i (fig. 4) indicates that the true values of loss coefficient would also show a systematic increase with δ^*_i/D_i. Since the maximum thickness of the boundary layer of these tests is about 20 percent of the maximum possible thickness (fully developed pipe flow) and the range of loss coefficients obtained consequently represents probably only a small part of the maximum range, the conclusion is reached that the loss coefficient of diffusers of the class investigated depends strongly on the relative thickness of the inlet boundary layer.

The effect of increasing flow quantity (increasing Reynolds and Mach number), as indicated by mutual consideration of both figures 4 and 5, ranges from no net effect for the thin boundary layer for the 12°,21-inch diffuser to very strong adverse effects for the thick boundary layer for the 12°,10-inch diffuser and the 23° diffuser. For the 23° diffuser, the measured loss coefficient was increased approximately 50 percent by increasing the inlet Mach number from 0.30 to 0.55, and the corrected loss coefficients would show considerably more increase.

In an analysis of these results, a review of some of the known effects of the factors involved will be helpful. Increasing Reynolds number, as shown in reference 8, has a detrimental effect on boundary-layer development, as has increasing Mach number, which increases the nondimensional pressure gradient. Therefore, in the 23° diffuser, in which the boundary layer develops rapidly because of the wide diffuser angle, both the Reynolds number and Mach number effects are large. Friction losses, however, decrease with increasing Reynolds number, so that in the 12° diffusers, in which friction constitutes a significant part of the losses, the adverse effects of Reynolds and Mach number on boundary-layer development and the favorable effect of Reynolds number on friction losses produce only a small net effect with increasing flow quantity (increasing Reynolds number and Mach number). Futhermore, since these effects are boundary-layer effects, in each diffuser the effects are stronger where the boundary layer constitutes a larger portion of the total flow.

The limiting inlet Mach number (choking Mach number) was reached in the 12° diffusers for all inlet pipe lengths, and the results indicate that the choking Mach number decreases continuously with increasing boundary-layer thickness. The data for the 23° diffuser do not extend to choking Mach numbers; however, the values probably would be approximately the same for this diffuser as for the 12°,21-inch diffuser for corresponding boundary-layer thicknesses.

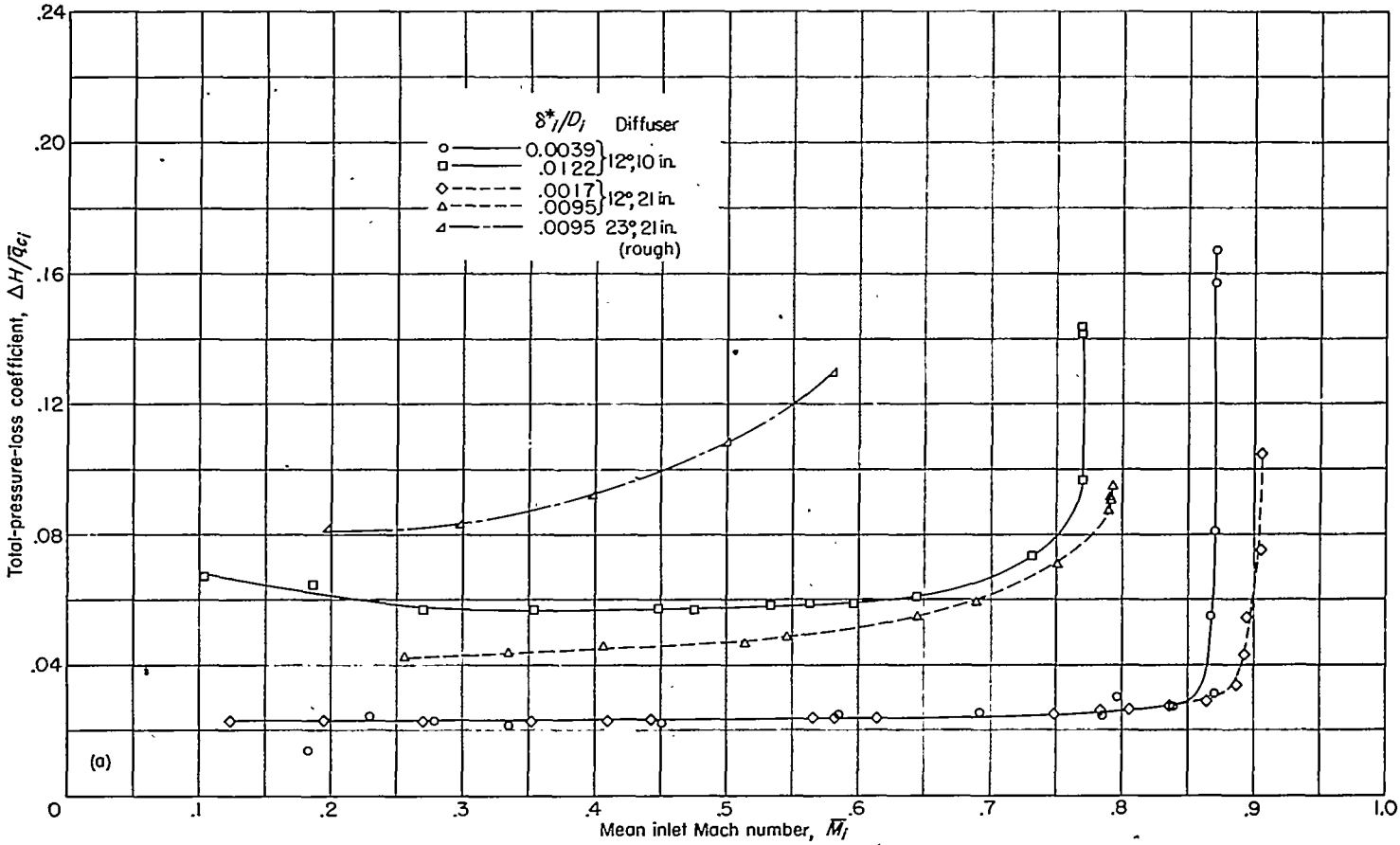

(a) Measured at diffuser exit.

FIGURE 5.—Variation of total-pressure-loss coefficient with Mach number.

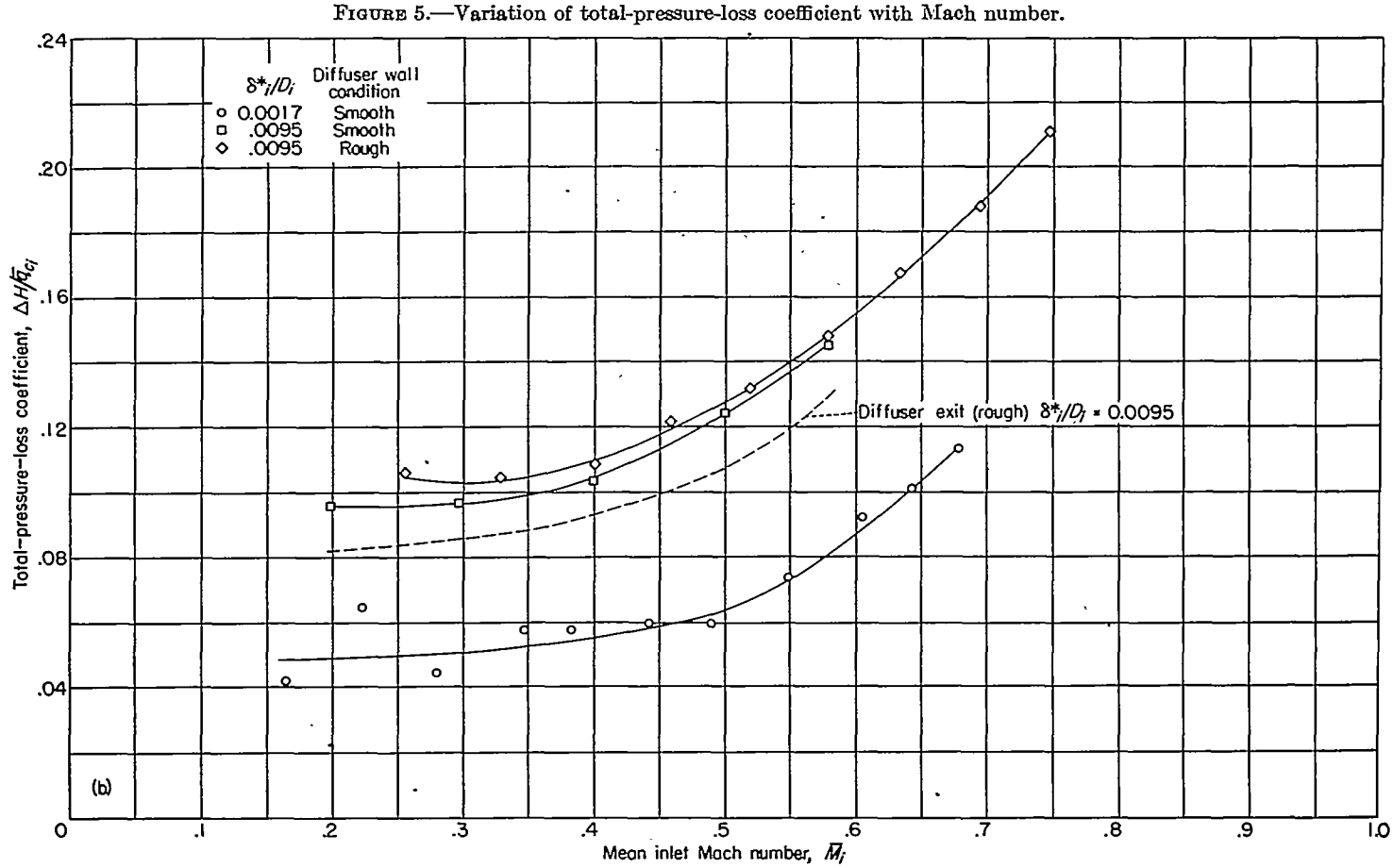

(b) Measured at 23°,21-inch tailpipe exit.

FIGURE 5.—Concluded.

For the 23° diffuser, the curves of $\frac{\Delta H}{\overline{q}_{c_i}}$ plotted against $\overline{M}_i$ in figure 5 (b) show approximately the same effects of flow rate and inlet-boundary-layer thickness for measurements at the tailpipe exit as were noted for measurements at the diffuser exit. Comparison with the diffuser-exit curve for the 23°,21-inch diffuser, which is plotted in figure 5 (b) as a reference, shows that the loss coefficient at the end of the tailpipe was about 15 percent higher than at the end of the diffuser over the range of flows investigated; and, as was pointed out previously, roughening the walls of the diffuser had little effect on $\frac{\Delta H}{\overline{q}_{c_i}}$.

Diffuser effectiveness.—The diffuser-effectiveness parameter $\Delta p/\Delta p_{ideal}$ is plotted against mean inlet Mach number for the two 12° diffusers and the 23° diffuser in figure 6. At a given inlet Mach number, continuously decreasing effectiveness is obtained by increasing inlet-boundary-layer thickness or diffuser angle, which is in agreement with trends observed in the loss-coefficient results. The data exhibit a tendency for the effectiveness to increase slightly as the inlet Mach number is increased up to a value of about 0.4. Increasing the Mach number beyond this point produces a continuous loss in diffuser effectiveness. The severity of the depreciation increases systematically with increasing boundary-layer thickness or diffuser-expansion angle, as would be expected. The magnitudes of the effects are roughly the same as the changes in loss coefficient.

STATIC-PRESSURE DISTRIBUTION

Distributions of pressure ratio p/H_0 through the diffusers are plotted in figure 7. In each part of this figure, distributions for the thinner inlet boundary layer are compared with those for the thicker inlet boundary layer. The curves for the thinner inlet-boundary-layer condition are determined by actual data points, which have been omitted for clarity, and curves for the thicker inlet-boundary-layer condition which match the inlet static-pressure ratios of the thinner inlet-boundary-layer curves were obtained by cross-plotting and interpolating the original data. The general pattern is the same for all results. A local acceleration of the flow, as

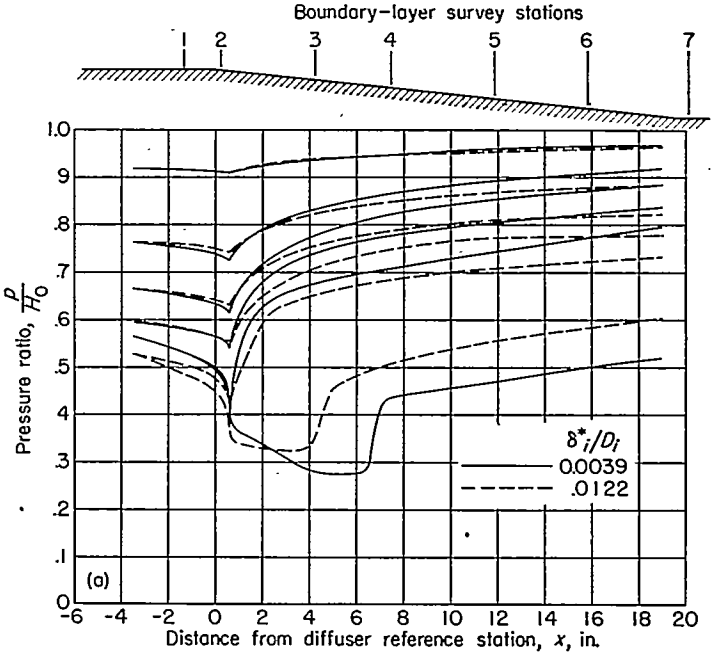

(a) 12°,10-inch diffuser.

FIGURE 7.—Comparison of distributions of nondimensionalized static pressures.

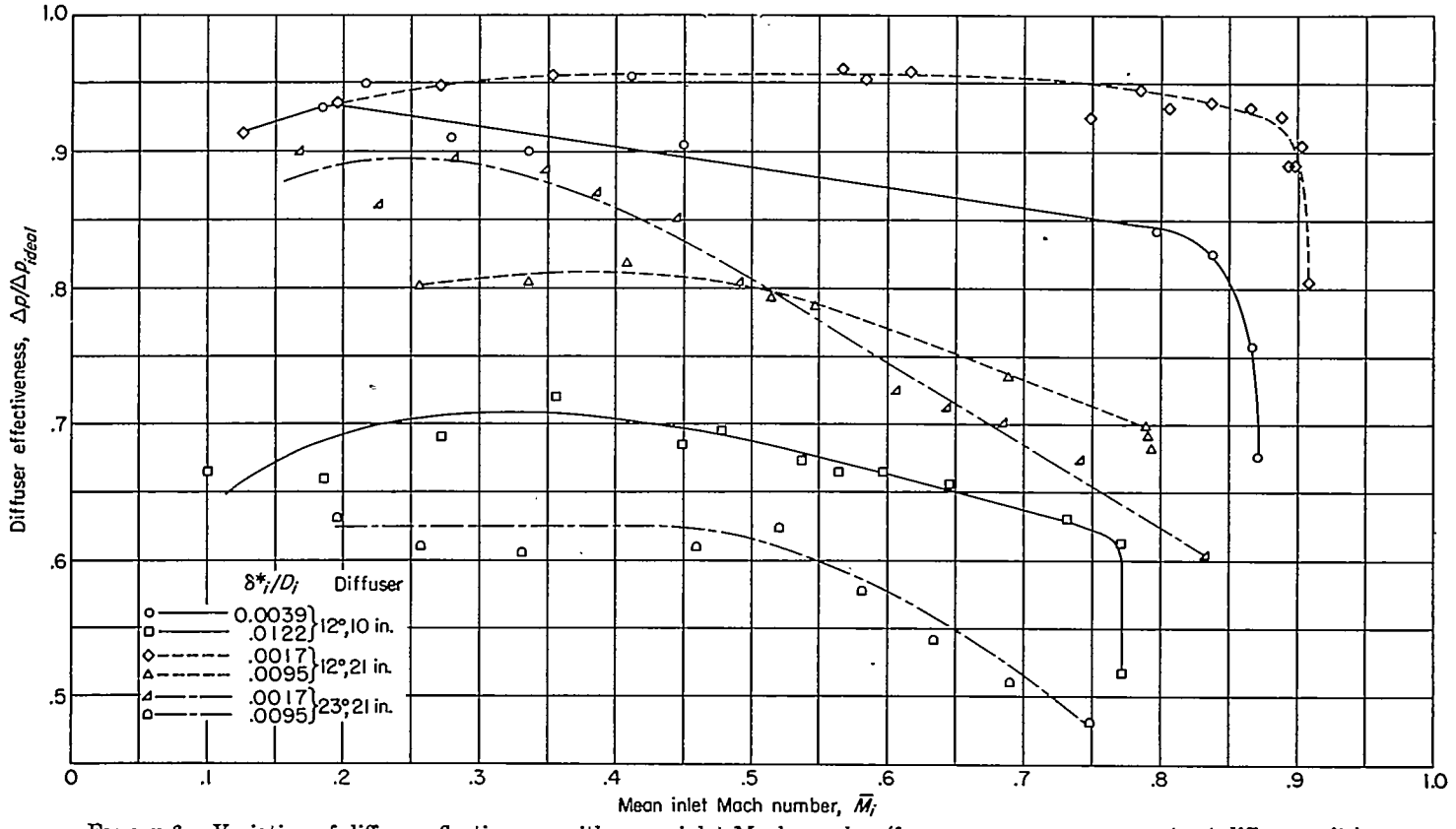

FIGURE 6.—Variation of diffuser effectiveness with mean inlet Mach number (from pressure measurements at diffuser exits).

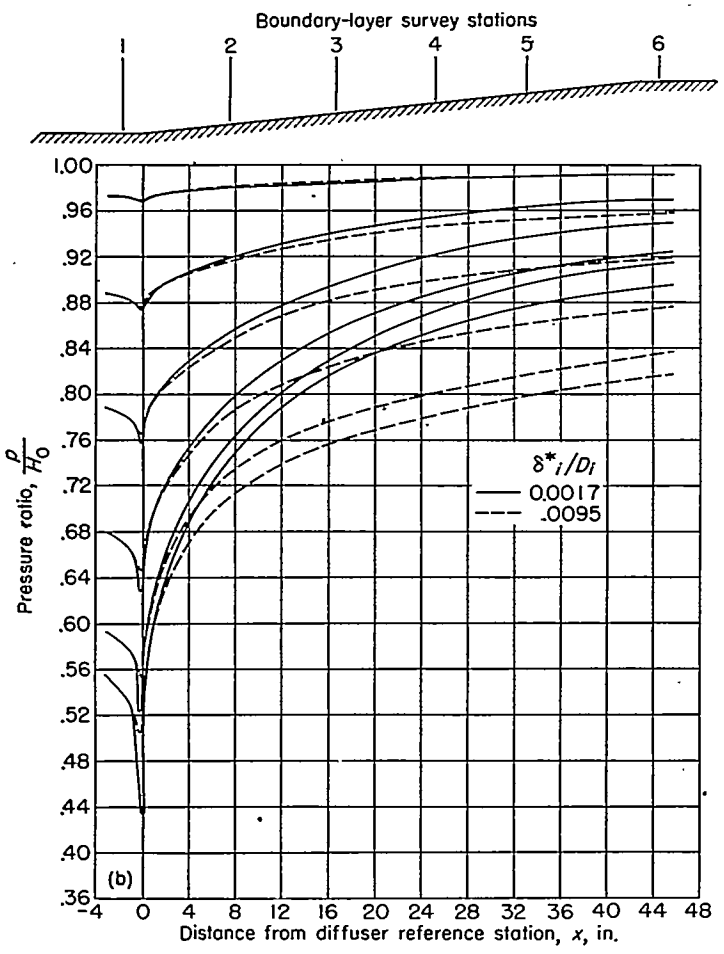

(b) 12°,21-inch diffuser.

FIGURE 7.—Continued.

indicated by decreasing values of p/H_0, occurs ahead of and in the region of the transition-section curvature. The peak of this acceleration (minimum pressure) occurs slightly downstream of the midpoint of the transition arc and is followed by a deceleration and corresponding rise in p/H_0 as the flow starts to expand in the diffuser. The severity of pressure gradients in this transition section increases with increasing inlet Mach number and decreases with thickening of the inlet boundary layer. The flow deceleration and rise in p/H_0 continues through the diffuser and, as shown in figure 7 (c), into the tailpipe for the 23° diffuser. The effect of the thicker inlet boundary layer in reducing the pressure rise through the diffusers can be seen in each part of this figure.

BOUNDARY-LAYER RESULTS

Boundary-layer characteristics.—Boundary-layer velocity distributions were measured at a number of stations and at several values of inlet velocity in each diffuser. A large number of these velocity distributions are given in table II. Values of boundary-layer thickness δ, displacement thickness δ^*, boundary-layer shape parameter δ^*/θ, and momentum thickness θ were obtained from these and other velocity distributions and are given in table III.

As an aid in interpreting the boundary-layer results ob-

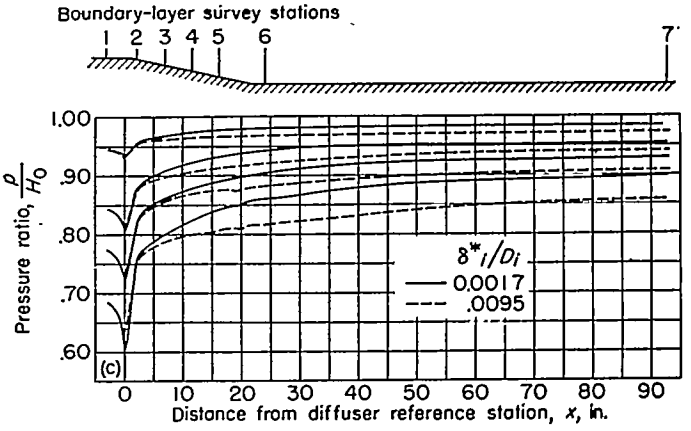

(c) 23°,21-inch diffuser.

FIGURE 7.—Concluded.

tained in this investigation, the physical interpretation of turbulent separation is briefly reviewed. When a stream proceeds into a region of increasing static pressure, the force due to the pressure gradient opposes the flow. Excess of this opposing force over the shear forces associated with transverse gradients of longitudinal velocity is balanced by reduction in momentum of the fluid. Equilibrium of forces is achieved, therefore, by a retardation of the flow. When the momentum of the fluid is insufficient to establish equilibrium, separation results. Separated flow is usually quite unstable, and the conditions are seldom, if ever, either steady or uniformly distributed about the perimeter of even the most nearly symmetrical channel so that no clearly defined point of separation exists but the separation phenomena extends instead over a zone.

Velocity profiles of a boundary layer subjected to an adverse pressure gradient are distorted by the local retardations and flow reversals which occur. Typical profiles of u/U plotted against the distance from the wall y are shown in figure 8. Profile A is representative of a boundary-layer flow at constant pressure. Profile B is an example of clearly separated flow obtained in a region of adverse pressure gradient. Profiles C and D are typical of those encountered in regions of adverse pressure gradient in which actual reversal has not yet been observed, at least at the point on the circumference at which the profile was measured. The appearance of either profile C or D suggests that separation is imminent or has occurred elsewhere on the circumference. As is shown subsequently, profile D, which is of particular interest because of the appearance of a high velocity very close to the wall, may be obtained simultaneously with profile C at the same longitudinal position in a symmetrical diffuser but at a point somewhat removed circumferentially. Precise determination of the point of initial separation of flow in an adverse pressure gradient presents much difficulty because of the appearance of asymmetry in the flow pattern. Although observation of a profile such as profile B clearly establishes separation, failure to observe such a profile cannot be taken unreservedly as proof of the absence of separation but merely indicates that separation has not occurred at the point on the circumference at which the measurements were made.

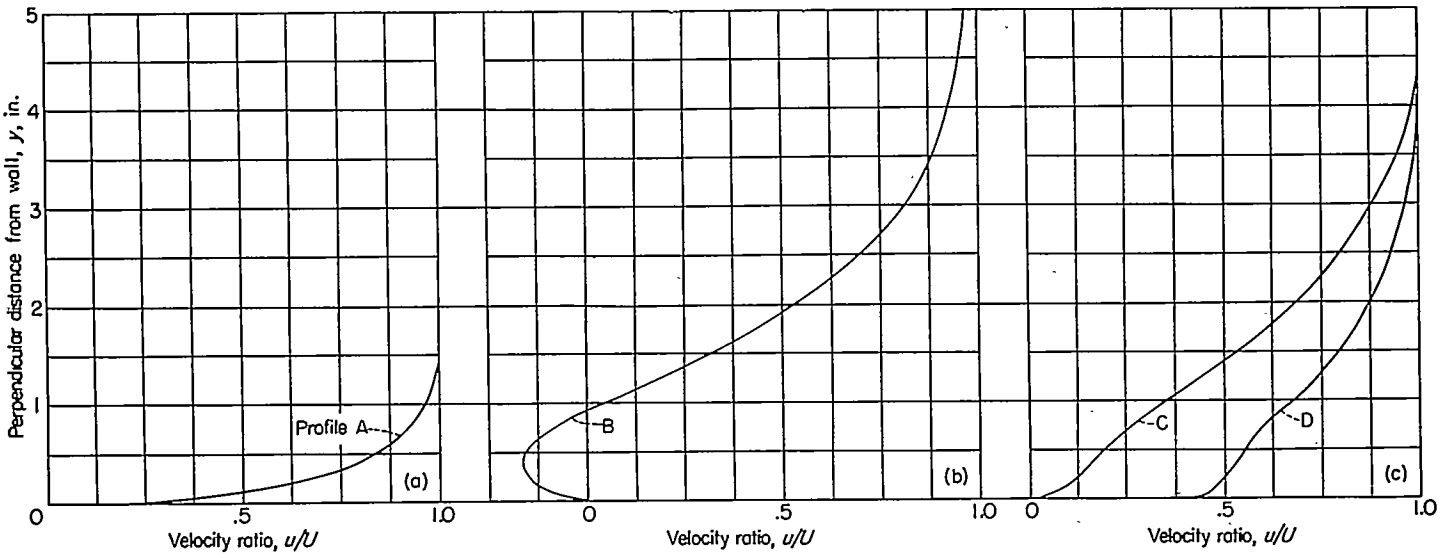

(a) Normal, zero-pressure-gradient, turbulent-boundary-layer profile.

(b) Separated-flow profile.

(c) Turbulent-boundary-layer profiles in adverse pressure gradient indicative of imminent separation.

FIGURE 8.—Turbulent-boundary-layer velocity profiles.

Since the shape of the velocity profile is indicative of the condition of the boundary layer, the numerical value of the shape parameter derived from the profile bears a definite relationship to the approach of the separation point. It is shown by Von Doenhoff and Tetervin (ref. 9) from two-dimensional data that the shape of a large class of turbulent-boundary-layer profiles can be expressed, with fair accuracy, as a function of a single parameter, the ratio of the boundary-layer displacement thickness δ^* to the momentum thickness θ. It is stated in reference 9 that separation was never observed at a value of δ^*/θ less than 1.8 and appears definitely to have occurred for shape-parameter values greater than 2.6. It is further explained that it is impossible to fix these values accurately because the turbulent separation point is not clearly defined.

The 12°,10-inch diffuser.—Inlet-boundary-layer profiles in the 12°,10-inch diffuser for three different values of p_i/H_0 are plotted nondimensionally in figure 9. This figure reveals a striking difference in profile shape between the boundary layer for $\delta^*_i/D_i=0.0039$ and that for $\delta^*_i/D_i=0.0122$. For $\delta^*_i/D_i=0.0122$, the profile shape is that of a fully developed turbulent flow as illustrated in figure 8, profile A. For $\delta^*_i/D_i=0.0039$, however, the profile has an irregular shape more like profiles C and D of figure 8 in which velocity and momentum deficiencies exist near the wall. From the preceding discussion of boundary-layer separation, it would be expected that this thinner boundary layer will separate much more easily than the thicker one. The reason for the existence of this profile is not known, although it is believed to be associated with incomplete transition from laminar to turbulent flow. No attempt to correct the situation was made since this irregularity was not discovered until the test program had been completed.

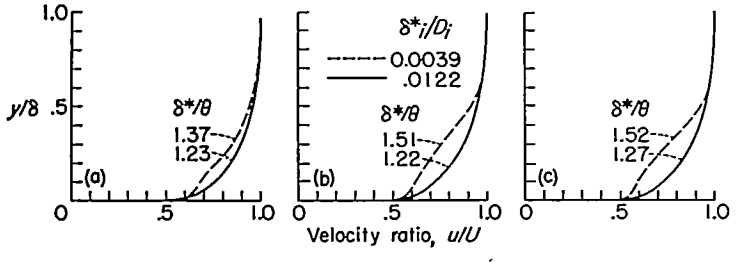

(a) $\frac{p_i}{H_0}=0.96$. (b) $\frac{p_i}{H_0}=0.60$. (c) $\frac{p_i}{H_0}=0.53$.

FIGURE 9.—Comparison of nondimensional velocity profiles at boundary-layer station 1 for 12°,10-inch diffuser.

The growth and behavior of the boundary layer in the 12°,10-inch diffuser is illustrated in figure 10, where δ, δ^*, θ, and δ^*/θ are plotted against x for both $\delta^*_i/D_i=0.0039$ and $\delta^*_i/D_i=0.0122$. For $\delta^*_i/D_i=0.0122$, the growth of all the parameters is smoothly and continuously dependent upon distance downstream and p_i/H_0 except that the shape-factor growth increases in the strong adverse pressure gradient at the diffuser inlet. There is a small region of separation near the inlet at low values of p_i/H_0 (high inlet velocities) and another at station 7 at the extreme high value of p_i/H_0 (extreme low inlet velocity). For $\delta^*_i/D_i=0.0039$, the effect of the poor inlet-boundary-layer shape overshadows the effect of inlet-boundary-layer thickness. The general effects of p_i/H_0 and x are the same as for $\delta^*_i/D_i=0.0122$, but they are considerably accentuated by the initial boundary-layer distortion. At low velocities, the boundary layer does not separate except near the exit, but at high velocities ($p_i/H_0 \leq 0.63$) the boundary layer separates at the inlet and, except for a small region of re-attachment when $p_i/H_0=0.63$, remains separated through most of the diffuser. Separated flow does not necessarily lead to high diffuser losses, but it does directly affect the significant expansion of the flow, thereby affecting the static-pressure recovery. A re-examination of figure 6 shows that a considerable decrease in $\Delta p/\Delta p_{ideal}$ accompanies the rapid growth of δ^* and increase of separation with increasing inlet Mach number.

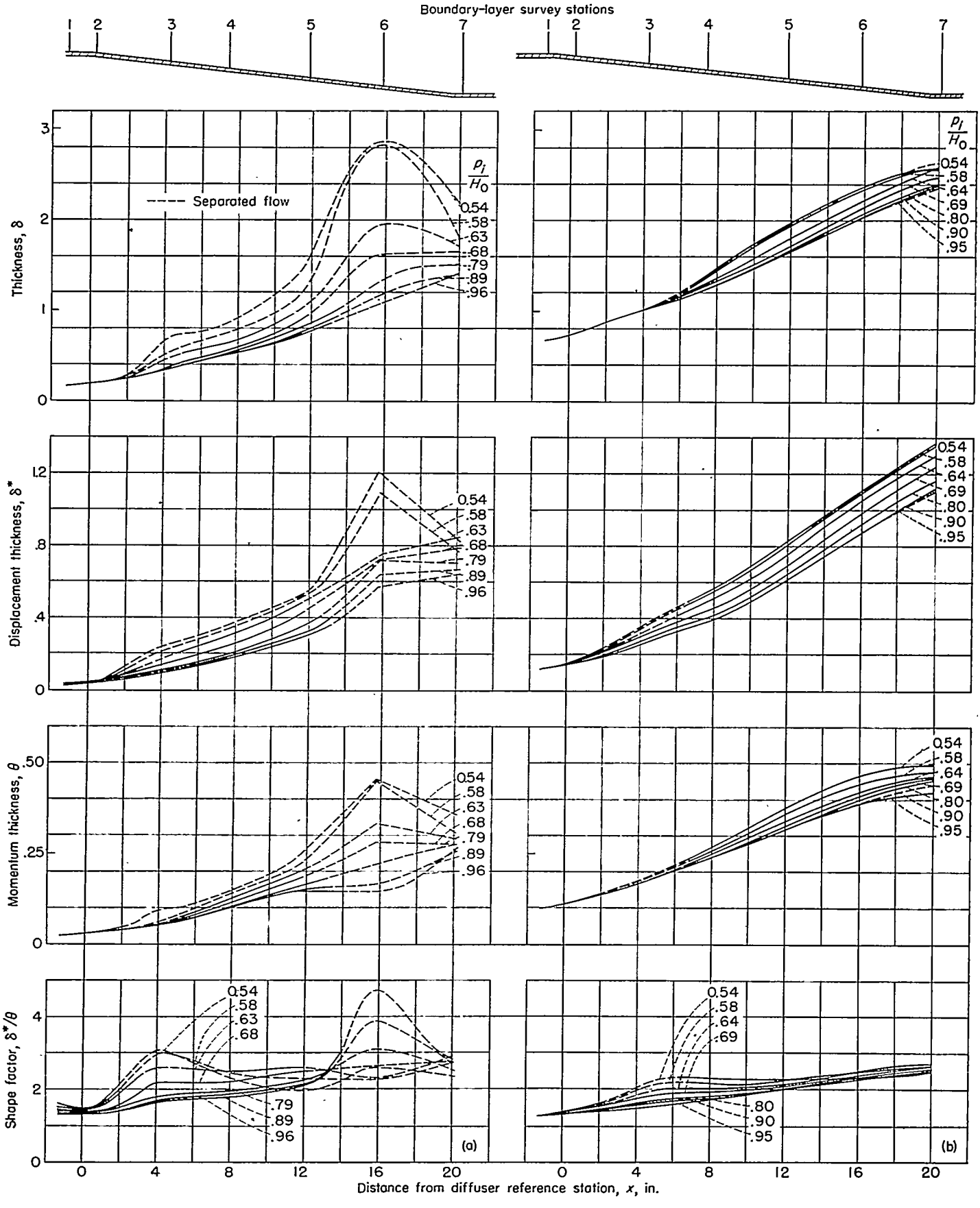

(a) $\frac{\delta^*_i}{D_i}$=0.0039. (b) $\frac{\delta^*_i}{D_i}$=0.0122.

FIGURE 10.—Growth of boundary-layer parameters in the 12°,10-inch diffuser.

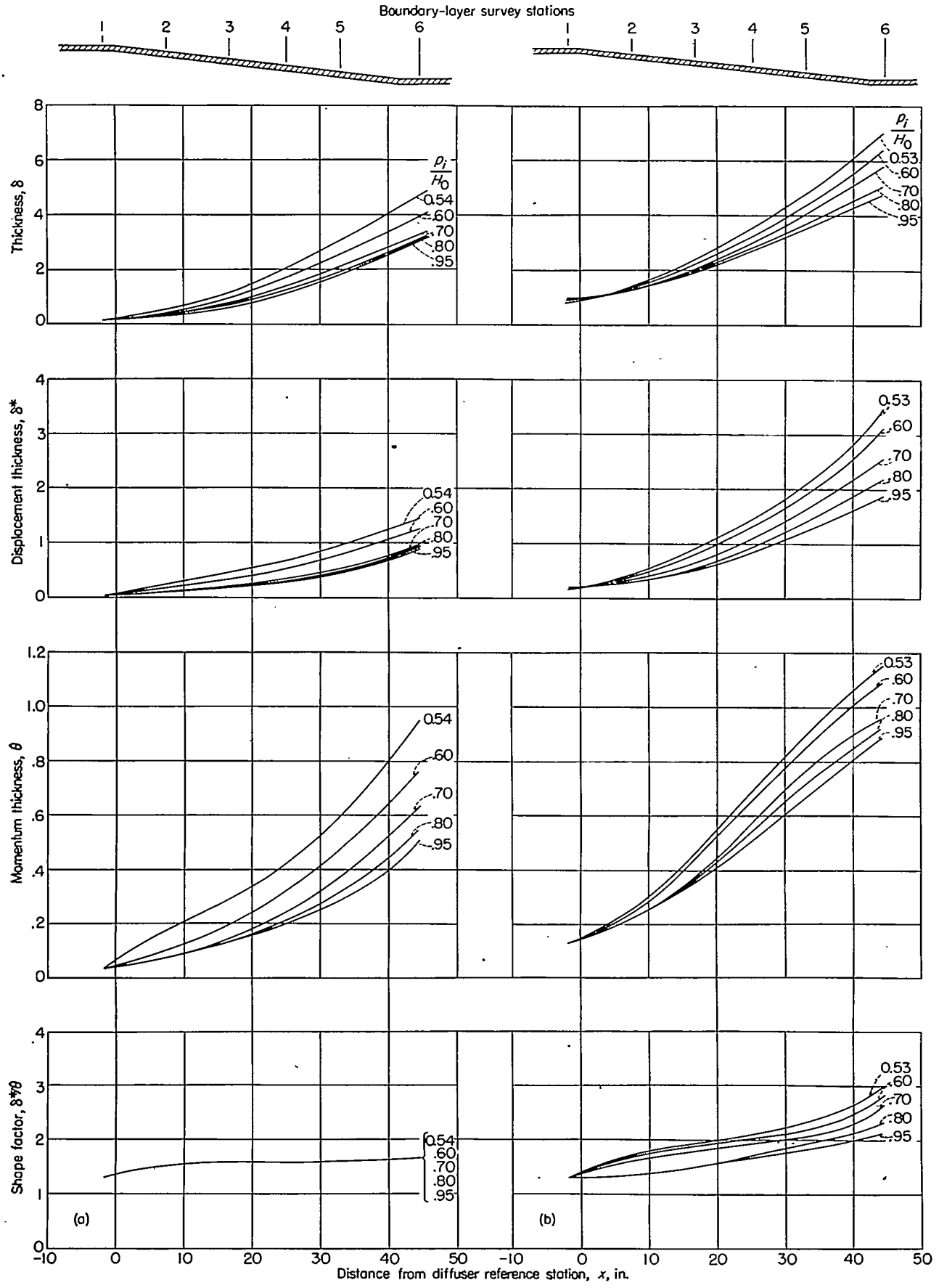

(a) $\frac{\delta^*_i}{D_i}$=0.0017. (b) $\frac{\delta^*_i}{D_i}$=0.0095.

FIGURE 11.—Growth of boundary-layer parameters in the 12°,21-inch diffuser.

368555—56——66

The 12°,21-inch diffuser.—Inlet-boundary-layer profiles for the 12°,21-inch diffuser were of the normal turbulent-flow type for both $\delta^*_i/D_i=0.0017$ and $\delta^*_i/D_i=0.0095$. The parameters δ, δ^*, θ, and δ^*/θ are plotted against x for this diffuser in figure 11. For both inlet-boundary-layer conditions, boundary-layer growth proceeds in an orderly fashion through the diffuser with no evidence of separation in the plane of these measurements. Boundary-layer thicknesses increase with increasing distance downstream and with increasing inlet velocity. The shape factor for $\delta^*_i/D_i=0.0017$ is unaffected by inlet velocity and increases only slightly with distance. This result is obtained also at low inlet velocities for $\delta^*_i/D_i=0.0095$, but in this case the rate of growth of shape factor increases with increasing inlet velocity.

Boundary-layer profiles, measured at points 120° apart around the diffuser-exit periphery at the highest inlet velocity, are shown in figure 12 for $\delta^*_i/D_i=0.0017$ and in figure 13 for $\delta^*_i/D_i=0.0095$. For $\delta^*_i/D_i=0.0017$, the flow is uniformly distributed over the diffuser surface, but for $\delta^*_i/D_i=0.0095$, attached flow was observed at two points and separated flow at the third. The absence of separation in figure 11, therefore, does not necessarily mean that there was no separation outside the plane of measurement. The data indicate, however, that separation was probably confined to small regions near the diffuser exit.

The 23°,21-inch diffuser.—Inlet-velocity profiles for the 23°,21-inch diffuser were the same as those for the 12°,21-inch diffuser. Boundary-layer parameters δ, δ^*, θ and δ^*/θ for this diffuser are plotted against x in figure 14. The peculiar increase and then decrease of boundary-layer thickness at the higher inlet velocities (lower p_i/H_0) for $\delta^*_i/D_i=0.0017$ probably is caused by separation occurring outside the measuring plane in such a way as to permit the boundary layer along the measuring plane to re-establish itself. For $\delta^*_i/D_i=0.0095$, the boundary-layer parameters indicate that separation is extensive downstream of station 3. In the 12° diffusers, the increases in boundary-layer thickness were not sufficient to change the flow pattern considerably, but, for this 23° diffuser, the increase in boundary-layer thickness does have a marked effect on boundary-layer action.

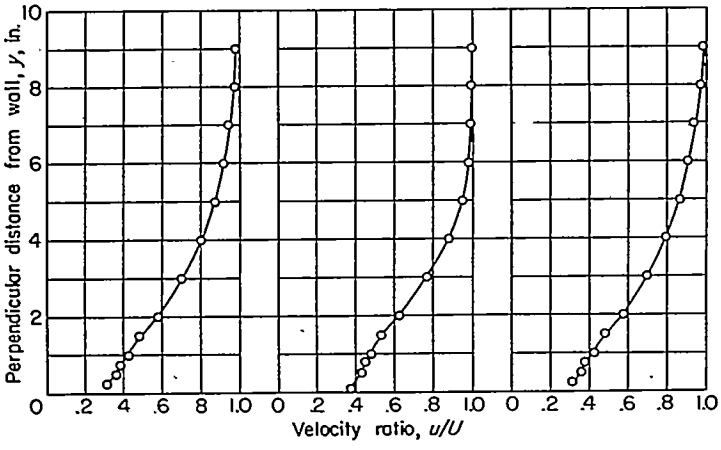

FIGURE 12.—Boundary-layer profiles 120° apart at the exit of the 12°,21-inch diffuser. $\frac{\delta^*_i}{D_i}=0.0017$; $\frac{p_i}{H_0}=0.54$.

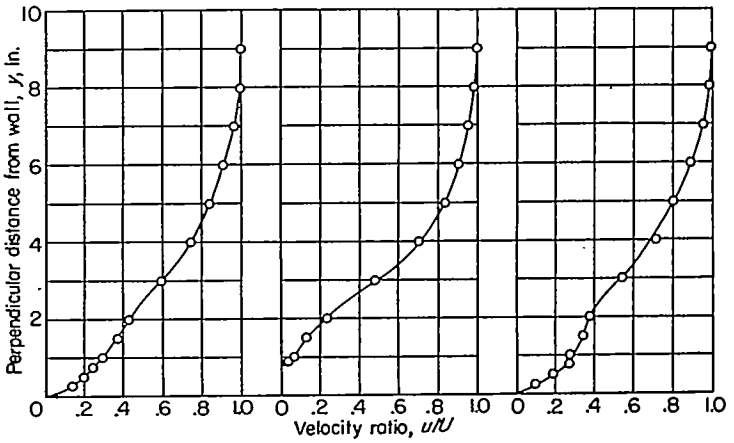

FIGURE 13.—Boundary-layer profiles 120° apart at the exit of the 12°,21-inch diffuser. $\frac{\delta^*_i}{D_i}=0.0095$; $\frac{p_i}{H_0}=0.55$.

Profiles from points 120° apart around the diffuser-exit periphery are plotted in figure 15 for $\delta^*_i/D_i=0.0017$ and in figure 16 for $\delta^*_i/D_i=0.0095$. These profiles show considerable asymmetry about the diffuser center line. For $\delta^*_i/D_i=0.0017$, one profile shows unmistakable separation, whereas the other two indicate that separation is imminent, especially at the higher inlet velocity. For $\theta^*_i/D_i=0.0095$, the situation is worse with two clearly separated profiles and one attached. In figure 17 are plotted profiles which were measured at the same points at two different times. These profiles were taken at stations 2 and 5 for $\delta^*_i/D_i=0.0095$. They show that, at station 2, both separated and unseparated flow profiles were observed at different times. The nature of separated flow in large-angle conical diffusers, therefore, appears to be asymmetric, unstable, and unpredictable.

The effectiveness of roughness in stabilizing the flow of the 23° diffuser is shown in figure 18. These typical exit-velocity profiles are shown for varying amounts of diffuser surface roughened, as indicated. The pressure measurements from which these velocities were computed were extremely steady. Observation of the flow by means of tufts attached to the wall did not reveal any regions of separated flow.

CONCLUSIONS

From the data obtained for values of inlet-boundary-layer displacement thickness ranging from very small values up to about 20 percent of the maximum possible value (fully developed pipe flow) in 12° and 23° conical diffusers having ratios of exit area to inlet area of 2.0, the following conclusions are drawn:

1. The performance in terms of total-pressure-loss coefficient and diffuser effectiveness was strongly dependent on inlet-boundary-layer thickness and diffuser expansion angle. Systematic depreciation in performance was obtained with increasing values of these variables.

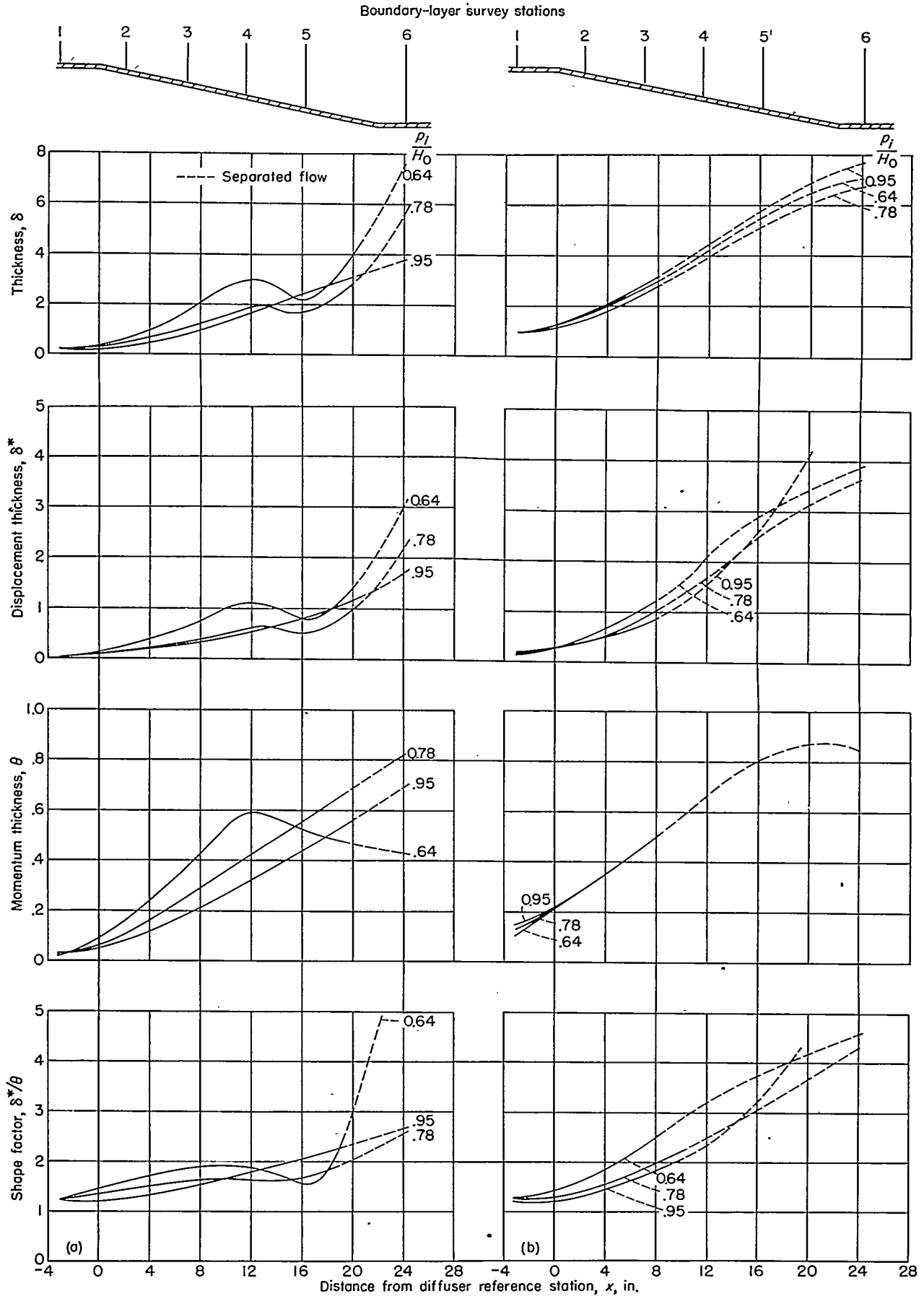

(a) $\frac{\delta^*_i}{D_i}$=0.0017. (b) $\frac{\delta^*_i}{D_i}$=0.0095.

FIGURE 14.—Growth of boundary-layer parameters in the 23°,21-inch diffuser.

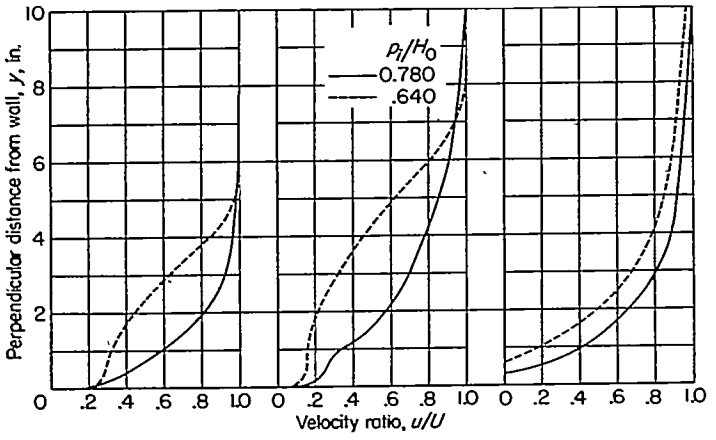

FIGURE 15.—Boundary-layer profiles 120° apart at the exit of the 23°,21-inch diffuser for $\frac{\delta^*_i}{D_i}$=0.0017.

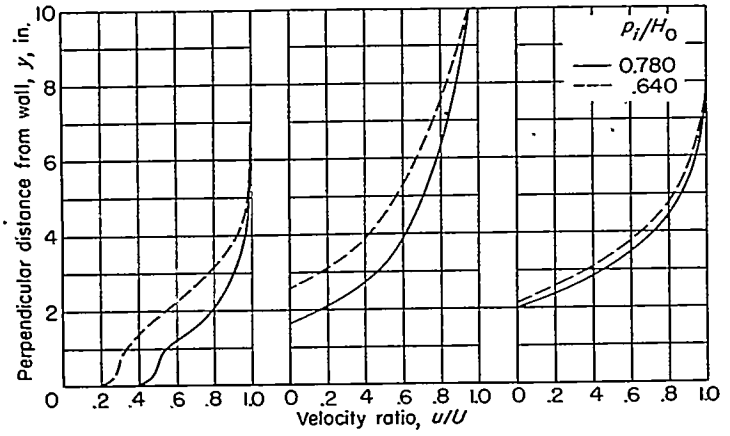

FIGURE 16.—Boundary-layer profiles 120° apart at the exit of the 23°,21-inch diffuser for $\frac{\delta^*_i}{D_i}$=0.0095.

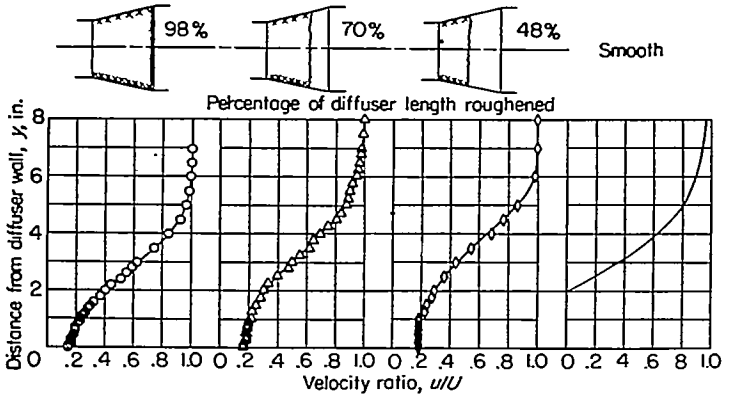

FIGURE 18.—Comparison of exit-velocity profiles for roughened and smooth 23°,21-inch diffuser.

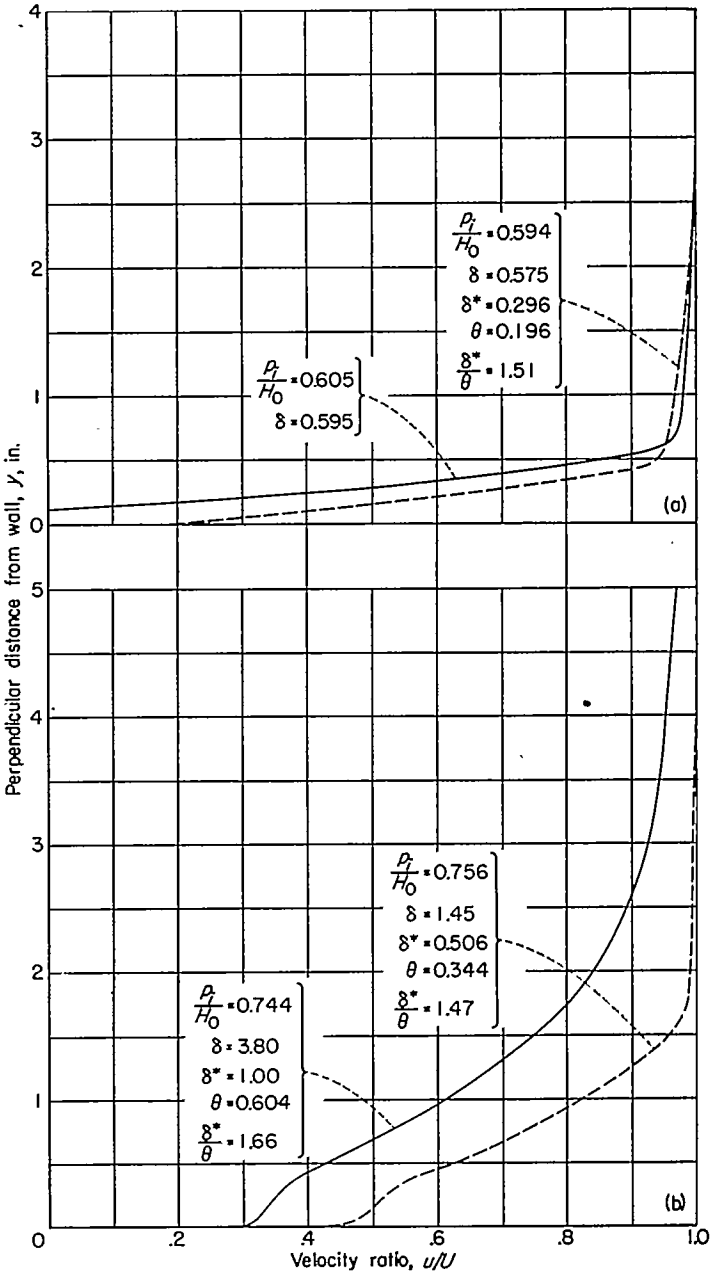

(a) Station 2.
(b) Station 5.

FIGURE 17.—Comparison of boundary-layer profiles measured at the same point at different times in the 23°,21-inch diffuser for $\frac{\delta^*_i}{D_i}$=0.0095.

2. The adverse effects of increasing flow rate (increasing inlet Mach and Reynolds numbers) upon performance ranged from no effect for the thinnest inlet-boundary-layer condition to very strong effects for the thickest inlet-boundary-layer condition. The severity of these effects also increased progressively with increasing diffuser angles.

3. The existence of a distorted inlet-boundary-layer-profile shape for the thinner inlet boundary layer of the 12°,10-inch diffuser resulted in some flow separation at nearly all inlet Mach numbers. This unusual flow pattern obscured the effects of inlet-boundary-layer thickness in that diffuser. In the 12°,21-inch diffuser, only a small region of separated flow was observed at the highest inlet Mach number.

4. In the 23°,21-inch diffuser, the flow was separated over the major portion of the diffuser for all Mach numbers and was so unsteady that reliable transverse pressure surveys could not be made near the diffuser exit. When the diffuser surface was uniformly roughened by applying 0.10-inch-diameter particles of cork, the flow was made steady throughout the flow range investigated. This roughness did not significantly affect the performance.

5. Observations at different points around the diffuser peripheries revealed that the separated flow pattern was not symmetrical about the center line, and furthermore, that the regions of separated flow shifted with time.

LANGLEY AERONAUTICAL LABORATORY,
NATIONAL ADVISORY COMMITTEE FOR AERONAUTICS,
LANGLEY FIELD, VA., *November 15, 1954.*

REFERENCES

1. Gibson, A. H.: On the Flow of Water Through Pipes and Passages Having Converging or Diverging Boundaries. Proc. Roy. Soc. (London), ser. A, vol. 83, no. 563, March 2, 1910, pp. 366–378.
2. Peters, H.: Conversion of Energy in Cross-Sectional Divergences Under Different Conditions of Inflow. NACA TM 737, 1934.
3. Kröner, Richard: Versuche über Strömungen in stark erweiterten Kanälen. Forsch.-Arb. Geb. Ing.-Wes. VDI-Verlag G.m.b.H. (Berlin), Heft 222, 1920, pp. 1–85.
4. Vedernikoff, A. N.: An Experimental Investigation of the Flow of Air in a Flat Broadening Channel. NACA TM 1059, 1944.
5. Jones, R., and Williams, D. H.: The Effect of Surface Roughness on the Characteristics of the Aerofoils N.A.C.A. 0012 and R.A.F. 34. R. & M. No. 1708, British A.R.C., 1936.
6. Persh, Jerome: The Effect of Surface Roughness on the Performance of a 23° Conical Diffuser at Subsonic Mach Numbers. NACA RM L51K09, 1952.
7. Persh, Jerome, and Bailey, Bruce M.: A Method for Estimating the Effect of Turbulent Velocity Fluctuations in the Boundary Layer on Diffuser Total-Pressure-Loss Measurements. NACA TN 3124, 1954.
8. Rubert, Kennedy F., and Persh, Jerome: A Procedure for Calculating the Development of Turbulent Boundary Layers Under the Influence of Adverse Pressure Gradients. NACA TN 2478, 1951.
9. Von Doenhoff, Albert E., and Tetervin, Neal: Determination of General Relations for the Behavior of Turbulent Boundary Layers. NACA Rep. 772, 1943. (Supersedes NACA WR L–382.)

TABLE I.—LOCATION OF SURVEY STATIONS

(a) General Instrumentation

Quantity	Distance from reference station, x (positive downstream), in.		
	12°,10-inch diffuser	12°,21-inch diffuser	23°,21-inch diffuser
Diffuser-inlet total pressure and mass flow	−1.3	−4.1	−4.1
Diffuser-exit total pressure and mass flow	20.1	42.1	21.9
Reference total pressure	Settling chamber	Settling chamber	Settling chamber
Reference stagnation temperature	Settling chamber	Settling chamber	Settling chamber
Diffuser-inlet static pressure	−1.6	−3.2	−3.2
Diffuser-exit static pressure	19.4	45.4	25.3
Tailpipe-exit total pressure	----	----	92.7

(b) Boundary-Layer Measurements

Station	Distance from reference station, x, in.		
	12°,10-inch diffuser	12°,21-inch diffuser	23°,21-inch diffuser
1	−1.3	−1.8	−3.2
2	0.2	7.5	2.1
3	4.2	16.7	6.9
4	7.4	25.2	11.5
5	11.8	33.0	16.2
6	15.8	44.5	24.1
7	20.1	----------	92.7

TABLE II.—BOUNDARY-LAYER VELOCITY DISTRIBUTIONS

(a) 12°,10-Inch Diffuser; $\delta^*_d/D_1=0.0039$

y, in.	u/U				
	Station 1				
p_d/H_0=	0.964	0.710	0.630	0.597	0.537
0.015	0.667	0.630	0.600	0.581	0.559
.045	.733	.692	.663	.648	.633
.075	.794	.771	.751	.741	.736
.105	.845	.830	.820	.813	.818
.155	.944	.946	.948	.945	.954
.205	.983	.985	.988	.982	.981
.255	1.000	.998	1.000	1.000	1.000
.305	1.000	1.000	1.000	1.000	1.000
	Station 2				
p_d/H_0=	0.960	0.708	0.615	0.587	0.530
0.015	0.641	0.620	0.587	0.575	0.727
.045	.719	.689	.662	.649	.779
.075	.778	.763	.743	.734	.839
.105	.831	.825	.815	.810	.892
.155	.902	.904	.901	.899	.954
.205	.952	.965	.968	.970	.975
.255	.984	.992	.994	.995	.983
.305	.992	.998	.998	.999	.983
	Station 3				
p_d/H_0=	0.963	0.709	0.627	0.588	0.562
0.015	0.415	0.231	-----	-----	-----
.045	.467	.312	-----	-----	-----
.075	.525	.380	0.206	-----	-----
.105	.577	.448	.316	0.165	-----
.155	.703	.593	.482	.388	0.284
.205	.795	.713	.612	.535	.510
.255	.871	.814	.728	.645	.658
.305	.916	.891	.824	.748	.777
.355	.959	.942	.896	.834	.856
.605	.994	1.000	.998	.997	.990
.855	.994	1.000	.999	1.000	.998
1.105	.994	1.000	1.000	1.000	.986
1.355	.994	1.000	1.000	1.000	.976
	Station 4				
p_d/H_0=	0.961	0.705	0.618	0.581	0.524
0.015	0.306	0.217	0.091	0	-----
.045	.346	.244	.158	.121	-----
.075	.400	.292	.190	.172	-----
.105	.447	.333	.233	.230	-----
.155	.542	.413	.312	.317	0.138
.205	.632	.491	.380	.387	.069
.255	.702	.567	.442	.458	.138
.305	.766	.646	.507	.510	.183
.355	.816	.713	.572	.565	.240
.605	.993	.981	.907	.872	.599
.855	1.000	1.000	.997	.981	.923
1.105	1.000	1.000	.999	.995	.973

y, in.	u/U				
	Station 5				
p_d/H_0=	0.963	0.715	0.622	0.589	0.534
0.015	0.226	0.158	0.091	0.143	0.185
.075	.291	.207	.115	.167	.122
.135	.344	.256	.163	.218	.113
.385	.624	.473	.366	.398	.153
.635	.873	.710	.576	.594	.257
.885	.992	.936	.834	.822	.413
1.135	.992	.993	.955	.920	.596
1.385	.992	.999	.988	.974	.783
1.635	.992	1.000	.998	.990	.882
1.85	.992	1.000	1.000	.996	.932
	Station 6				
p_d/H_0=	0.926	0.712	0.633	0.593	0.514
0.015	-----	0.151	0.145	0.141	-----
.075	-----	.126	.170	.118	-----
.135	-----	.145	.233	.184	-----
.385	0.205	.275	.325	.264	-----
.635	.533	.423	.468	.370	0.023
.885	.801	.604	.625	.491	.238
1.135	.946	.752	.744	.612	.375
1.385	1.000	.877	.846	.716	.520
1.635	1.000	.940	.916	.781	.639
1.85	1.000	.976	.941	.828	.735
	Station 7				
p_d/H_0=	0.961	0.783	0.627	0.590	0.529
0.05	0.147	0.088	-----	-----	-----
.10	.147	.125	-----	-----	-----
.20	.255	.216	0.191	0.211	-----
.50	.417	.380	.344	.405	0.062
1.00	.722	.683	.637	.669	.243
1.50	.967	.944	.885	.904	.450
1.75	.989	.970	.956	.954	.595
2.0	1.000	.996	.989	.992	.675
3.0	1.000	.998	.999	.998	.972
4.0	1.000	1.000	1.000	1.000	.986
5.0	1.000	1.000	1.000	1.000	.950
6.0	1.000	1.000	1.000	1.000	.890
7.05	1.000	1.000	1.000	1.000	.876

TABLE II.—BOUNDARY-LAYER VELOCITY DISTRIBUTIONS—Continued

(b) 12°,10-Inch Diffuser; $\delta^*/D_1=0.0122$

y, in.	u/U				
Station 1					
p_d/H_0=	0.954	0.753	0.608	0.545	0.518
0.015	0.621	0.623	0.584	0.550	0.565
.075	.707	.712	.682	.661	.676
.155	.780	.783	.763	.751	.765
.305	.840	.842	.831	.827	.835
.605	.928	.931	.928	.934	.937
.855	.976	.979	.980	.987	.984
1.105	.994	.996	.996	1.000	.997
1.355	.994	.996	.996	1.000	.997
1.605	.994	.996	.996	1.000	.997
Station 2					
p_d/H_0=	0.946	0.753	0.617	0.538	0.507
0.053	0.659	0.659	0.589	0.605	0.753
.113	.719	.792	.666	.682	.799
.208	.777	.780	.744	.760	.843
.428	.869	.871	.857	.868	.907
.783	.953	.962	.965	.968	.974
1.008	.984	.988	.990	.991	.988
1.268	.995	.997	.997	.997	.992
1.478	1.000	.999	.998	.997	.996
1.988	1.000	1.000	.998	.997	.996
Station 3					
p_d/H_0=	0.944	0.753	0.618	0.538	0.507
0.053	0.422	0.369	0.267	0.165	0.334
.113	.503	.450	.348	.270	.629
.208	.597	.561	.469	.416	.807
.428	.759	.736	.686	.654	.925
.783	.888	.887	.868	.869	.990
1.008	.940	.950	.940	.944	1.000
1.268	.979	.986	.983	.986	.986
1.478	.993	.995	.994	.995	.982
1.988	.993	.995	.994	.995	.970
Station 4					
p_d/H_0=	0.943	0.755	0.618	0.550	0.509
0.015	0.331	0.271	0.201	0.161	0.072
.075	.385	.334	.250	.216	0
.135	.415	.364	.278	.260	.072
.355	.593	.542	.450	.428	.280
.775	.810	.796	.741	.723	.696
1.0	.888	.884	.853	.843	.845
1.47	.968	.977	.974	.969	.968
1.74	.992	.977	.990	.990	.982
1.98	.992	.977	.990	.990	.985

y, in.	u/U				
Station 5					
p_d/H_0=	0.945	0.740	0.620	0.537	0.509
0.015	0.216	0.231	0.198	0.203	0.172
.075	.290	.254	.198	.190	.127
.135	.273	.269	.212	.208	.133
.355	.410	.380	.307	.287	.195
.775	.627	.597	.514	.476	.382
1.0	.743	.720	.636	.596	.515
1.47	.891	.909	.858	.825	.799
1.74	.962	.965	.934	.908	.900
1.98	.986	.989	.968	.953	.950
Station 6					
p_d/H_0=	0.943	0.750	0.623	0.544	0.509
0.045	0.195	0.162	0.149	0.174	0.128
.200	.258	.220	.186	.219	.153
.50	.365	.308	.269	.302	.194
1.0	.577	.516	.462	.462	.370
2.0	.936	.919	.889	.860	.82
2.5	1.000	.989	.978	.969	.941
3.0	1.000	.998	.994	.987	1.000
4.0	1.000	.998	.998	1.000	.938
5.0	1.000	.998	.998	1.000	.898
6.65	1.000	1.000	1.000	1.000	.795
Station 7					
p_d/H_0=	0.974	0.755	0.620	0.546	0.507
0.045	0.158	0.097	0.053	0.159	0.143
.200	.168	.181	.129	.188	.180
.50	.274	.261	.210	.235	.202
1.0	.418	.403	.347	.382	.292
2.0	.852	.814	.768	.757	.683
2.5	.949	.970	.934	.943	.888
3.0	.987	.997	.985	.982	.991
4.0	1.000	1.000	.995	.995	.969
5.5	1.000	1.000	.998	.998	.899
7.05	1.000	1.000	1.000	1.000	.822

TABLE II.—BOUNDARY-LAYER VELOCITY DISTRIBUTIONS—Continued

(c) 12°,21-Inch Diffuser; δ^*_d/D_t=0.0017

y, in.	u/U				
Station 1					
p_d/H_0=	0.957	0.828	0.657	0.593	0.538
0.025	0.755	0.723	0.675	0.646	0.775
.050	.822	.833	.751	.806	.891
.10	.907	.920	.875	.886	.940
.20	.978	.988	.990	.985	.993
.50	.996	.996	.995	.993	.999
1.00	1.000	1.000	1.000	.993	1.000
2.00	1.000	1.000	1.000	.995	1.000
3.00	1.000	1.000	1.000	1.000	1.000
Station 2					
p_d/H_0=	0.956	0.827	0.647	0.599	0.540
0.025	0.453	0.352	0.555	0.500	-----
.050	.580	.550	.586	-----	-----
.10	.662	.702	.645	.576	0.523
.20	.817	.844	.788	.744	.676
.50	.961	.969	.965	.980	.953
1.00	.990	.990	.992	.986	.978
2.00	1.000	.997	1.000	.996	.990
3.00	1.000	1.000	1.000	.999	.998
4.00	1.000	1.000	1.000	1.000	1.000
Station 3					
p_d/H_0=	0.954	0.828	0.654	0.596	0.530
0.025	0.335	0.320	0.470	0.415	-----
.050	.450	.470	-----	-----	0.330
.10	.590	.590	.507	.480	-----
.20	.720	.721	.575	.553	.392
.50	.905	.922	.785	.735	.519
1.00	.984	.990	.983	.964	.770
2.00	.998	.998	.995	.995	.956
3.00	1.000	1.000	1.000	.999	.987
4.00	1.000	1.000	1.000	1.000	.996
Station 4					
p_d/H_0=	0.951	0.798	0.651	0.597	0.530
0.025	0.221	0.345	0.393	0.367	0.313
.050	.380	.455	-----	.398	-----
.10	.489	.523	.445	.415	.345
.20	.606	.595	.493	.446	.399
.50	.783	.739	.633	.584	.474
1.00	.925	.915	.836	.777	.685
2.00	.995	.993	.990	.980	.932
3.00	.996	1.000	.994	.991	.987
4.00	1.000	1.000	1.000	.995	.995
5.00	1.000	1.000	1.000	1.000	1.000
Station 5					
p_d/H_0=	0.948	0.800	0.655	0.593	0.537
0.025	0.111	0.230	0.584	0.473	-----
.050	.187	.325	-----	-----	-----
.10	.275	.410	.625	.510	0.452
.20	.380	.512	-----	-----	.480
.50	.585	.660	.706	.585	.516
1.00	.796	.808	.783	.702	.602
2.00	.967	.977	.915	.873	.786
3.00	.989	.995	.980	.967	.907
4.00	.997	1.000	.990	.983	.980
5.00	.999	1.000	.995	.995	.995
6.00	1.000	1.000	1.000	1.000	1.000
Station 6					
p_d/H_0=	0.949	0.800	0.658	0.598	0.534
0.025	-----	-----	-----	0.405	0.390
.050	0.220	0.100	0.115	-----	-----
.10	.310	.170	.160	.428	-----
.20	.395	.279	.228	.447	.400
.50	.507	.457	.375	.485	.427
1.00	.638	.637	.545	.547	.485
2.00	.826	.835	.760	.710	.627
3.00	.922	.923	.890	.849	.770
4.00	.988	.955	.957	.942	.879
5.00	1.000	.975	.983	.989	.946
6.00	1.000	.985	.989	.995	.985
7.00	1.000	.993	.991	.995	.992
9.00	1.000	1.000	1.000	1.000	1.000

(d) 12°,21-Inch Diffuser; δ^*_d/D_t=0.0095

y, in.	u/U				
Station 1					
p_d/H_0=	0.953	0.826	0.684	0.540	0.530
0.025	-----	0.645	0.640	0.637	0.652
.050	0.697	.693	.684	.682	.699
.10	.745	.744	.734	.740	.746
.20	.806	.797	.797	.803	.816
.50	.897	.890	.895	.900	.907
1.00	.958	.953	.960	.968	.977
2.00	.983	.996	.995	.995	.999
3.00	1.000	1.000	.998	1.000	1.000
Station 2					
p_d/H_0=	0.952	0.820	0.684	0.550	0.528
0.025	-----	0.451	0.424	0.299	0.235
.050	0.488	.480	-----	-----	.280
.10	.556	.545	.467	.353	.313
.20	.639	.635	.575	.463	.402
.50	.800	.795	.769	.702	.672
1.00	.923	.913	.908	.880	.875
2.00	.976	.984	.980	.978	.977
3.00	.996	.996	.997	.994	.995
4.00	1.000	1.000	1.000	1.000	1.000
Station 3					
p_d/H_0=	0.952	0.822	0.692	0.554	0.528
0.025	-----	0.356	0.257	0.212	0.177
.050	0.398	-----	.280	.233	.236
.10	.437	.405	.338	.258	.256
.20	.495	.454	.370	.284	.306
.50	.640	.596	.508	.370	.390
1.00	.817	.802	.720	.607	.627
2.00	.946	.950	.943	.895	.930
3.00	.985	.985	.987	.967	.985
4.00	.995	.997	.996	.985	.997
5.00	1.000	1.000	1.000	.994	1.000
Station 4					
p_d/H_0=	0.952	0.820	0.688	0.553	0.530
0.025	-----	0.254	0.165	0.106	0.186
.050	0.329	-----	.207	.137	.189
.10	.346	.300	.247	.173	.228
.20	.384	.345	.284	.205	.263
.50	.509	.443	.335	.273	.300
1.00	.675	.622	.490	.409	.439
2.00	.892	.887	.805	.712	.756
3.00	.963	.961	.937	.926	.922
5.00	.995	.995	.992	.975	.990
7.00	1.000	1.000	1.000	.995	.996
Station 5					
p_d/H_0=	0.952	0.822	0.688	0.546	0.533
0.025	-----	0.252	0.116	0.205	0.222
.050	0.287	-----	.166	.223	.237
.10	.325	.293	.194	.247	-----
.20	.372	.326	.241	.260	.283
.50	.438	.376	.267	.297	.314
1.00	.564	.489	.343	.358	.384
2.00	.790	.726	.602	.576	.629
4.00	.967	.962	.942	.942	.931
6.00	.997	.994	.990	.988	.990
8.00	1.000	1.000	.998	.997	1.000
Station 6					
p_d/H_0=	0.952	0.811	0.687	0.552	0.531
0.025	-----	0.107	0.068	-----	0.117
.050	0.227	.159	.086	-----	.156
.10	.267	.193	.102	-----	.190
.20	.306	.237	.118	-----	.194
.50	.343	.279	.126	-----	.217
1.00	.413	.350	.176	0.067	.266
2.00	.647	.553	.347	.230	.417
3.00	.810	.741	.596	.480	.596
5.00	.967	.960	.902	.833	.883
7.00	.996	.997	.990	.950	.986
9.00	1.000	1.000	1.000	1.000	1.000

TABLE II.—BOUNDARY-LAYER VELOCITY DISTRIBUTIONS—Concluded

(e) 23°, 21-Inch Diffuser; $\delta^*_i/D_i=0.0017$

y, in.	u/U				
Station 1					
p_d/H_0=	0.948	0.872	0.812	0.733	0.583
0.025	0.730	0.733	0.618	0.725	0.703
.10	.840	.853	.870	.885	.893
.20	.930	.970	.978	.983	.993
.30	.987	.990	.992	.992	.994
.40	.990	.996	.996	.997	.998
.60	.994	-----	.998	.997	-----
1.00	1.000	1.000	1.000	1.000	1.000
Station 2					
p_d/H_0=	0.915	0.784	0.740	0.644	0.605
0.10	0.786	0.719	0.501	0.219	0
.20	.921	.860	.747	.510	.280
.30	.964	.935	.860	.736	.527
.40	.986	.968	.931	.840	.740
.60	.996	.989	.970	.940	.952
.80	.997	.992	.981	.972	.975
1.00	1.000	.998	.988	.985	.986
2.00	1.000	1.000	.991	.991	.997
4.00	1.000	1.000	1.000	1.000	1.000
Station 3					
p_d/H_0=	0.958	0.876	0.745	0.643	0.602
0.10	0.358	0.329	0.393	0.319	0.211
.40	.757	.733	.721	.567	.341
.60	.911	.893	.831	.631	.532
.80	.961	.949	.910	.762	.636
1.00	.982	.970	.934	.850	.775
1.50	.989	.989	.960	.906	.938
2.00	.994	.996	.987	.972	.980
4.00	1.000	1.000	.998	.996	.996
6.00	1.000	1.000	1.000	1.000	1.000
Station 4					
p_d/H_0=	0.945	0.871	0.741	0.647	0.604
0.10	0.350	0.397	0.256	0.277	0.230
.50	.618	.637	.490	.385	.292
1.00	.880	.880	.702	.575	.446
1.50	.957	.962	.816	.775	.622
2.00	.982	.982	.884	.856	.808
3.00	.992	.990	.943	.952	.955
4.00	1.000	1.000	.982	.977	.986
6.00	1.000	1.000	1.000	1.000	1.000
Station 5					
p_d/H_0=	0.956	0.881	0.756	0.649	0.613
0.10	0.191	0.210	0.518	0.493	0.487
.50	.390	.364	.630	.592	.555
1.00	.650	.632	.841	.754	.627
1.50	.836	.827	.960	.917	.780
2.00	.927	.922	.984	.964	.900
3.00	.990	.975	.995	.986	.970
4.00	.998	.990	1.000	.990	.990
6.00	1.000	1.000	1.000	1.000	1.000
Station 6					
p_d/H_0=	0.925	0.886	0.739	0.647	0.604
0.10	-----	-----	-----	0.187	0.116
.50	-----	-----	-----	.171	.118
.70	0	0	-----	.175	.180
1.00	.319	.260	.010	.200	.416
2.00	.703	.683	.421	.412	.710
3.00	.900	.876	.689	.693	.884
6.00	.976	.972	.860	.830	.983
7.00	-----	-----	.938	.992	.990
8.00	.991	.989	.953	.933	.998

(f) 23°, 21-Inch Diffuser; $\delta^*_i/D_i=0.0095$

y, in.	u/U				
Station 1					
p_d/H_0=	0.951	0.833	0.777	0.720	0.632
0.10	0.728	0.747	0.750	0.748	0.736
.20	.776	.789	.800	.806	.792
.50	.880	.883	.892	.900	.888
.90	.936	.939	.951	.959	.953
1.50	.979	.972	.987	.985	.985
2.00	.986	.980	.997	1.000	.998
4.00	1.000	1.000	1.000	1.000	1.000
Station 2					
p_d/H_0=	0.950	0.831	0.768	0.708	0.627
0.10	0.462	0.457	0.430	0.370	0.302
.20	.627	.573	.583	.530	.430
.50	.770	.769	.766	.769	.697
.90	.877	.873	.860	.866	.846
1.50	.942	.952	.957	.944	.952
2.00	.967	.982	.982	.976	.980
4.00	1.000	1.000	1.000	1.000	1.000
Station 3					
p_d/H_0=	0.954	0.834	0.781	0.708	0.628
0.10	0.202	0.220	0.189	0.166	0.117
.50	.518	.455	.481	.357	.258
.90	.746	.700	.651	.600	.537
1.50	.870	.836	.800	.792	.770
2.00	.903	.900	.906	.889	.880
3.00	.970	.984	.974	.970	.970
5.00	1.000	1.000	.992	.996	.996
6.00	1.000	1.000	1.000	1.000	1.000
Station 4					
p_d/H_0=	0.951	0.827	0.771	0.719	0.632
0.10	-----	0.068	-----	0	-----
.20	-----	.173	0	.110	-----
.60	0.217	.233	.180	.190	0
1.00	.507	.380	.280	.313	.227
2.00	.766	.703	.630	.663	.610
3.00	.903	.894	.880	.857	.842
4.00	.930	.980	.953	.956	.940
6.00	.982	1.000	1.000	1.000	1.000
Station 5					
p_d/H_0=	0.953	0.825	0.760	0.710	0.630
0.10	-----	-----	-----	0	-----
.20	-----	0	0	.100	-----
.40	-----	.098	.060	.125	-----
1.00	0	.240	.157	.180	0
2.00	.449	.459	.412	.447	.332
3.00	.662	.706	.682	.690	.627
4.00	.842	.835	.846	.816	.836
6.00	.960	.965	.955	.970	.960
8.00	1.000	1.000	1.000	1.000	1.000
Station 6					
p_d/H_0=	0.919	0.849	0.757	0.716	0.632
1.50	-----	0	-----	0	-----
2.00	0	.192	0	.110	0
3.00	.312	.471	.497	.443	.353
4.00	.567	.660	.669	.710	.630
6.00	.910	.930	.953	.920	.913
8.00	.963	.983	1.000	1.000	1.000

TABLE III.—BOUNDARY-LAYER RESULTS

(a) 12°,10-Inch Diffuser; δ^*_i/D_i=0.0039

p_d/H_0	δ	δ^*	θ	δ^*/θ
Station 1				
0.976	0.14	0.029	0.023	1.28
.964	.16	.034	.025	1.37
.920	.16	.032	.026	1.24
.870	.16	.034	.026	1.35
.788	.16	.035	.026	1.36
.710	.16	.036	.026	1.37
.669	.16	.038	.027	1.42
.630	.16	.042	.027	1.54
.593	.16	.041	.028	1.49
.597	.16	.041	.027	1.51
.542	.16	.044	.028	1.55
.539	.16	.044	.028	1.55
.537	.16	.044	.028	1.58
.538	.15	.042	.028	1.52
.537	.15	.042	.027	1.52
Station 2				
0.977	0.18	0.032	0.026	1.25
.960	.20	.039	.029	1.36
.919	.20	.038	.029	1.33
.866	.20	.038	.029	1.33
.794	.19	.039	.029	1.32
.708	.19	.041	.029	1.40
.665	.19	.042	.030	1.40
.615	.19	.043	.030	1.42
.587	.19	.045	.031	1.44
.598	.18	.046	.031	1.46
.537	.18	.045	.030	1.49
.530	.15	.026	.021	1.24
.536	.15	.026	.020	1.32
.530	.15	.025	.020	1.22
.530	.15	.025	.020	1.24
Station 3				
0.990	0.29	0.089	0.052	1.70
.963	.34	.104	.061	1.70
.923	.35	.106	.062	1.73
.840	.34	.112	.062	1.82
.787	.35	.118	.063	1.88
.709	.37	.135	.065	2.08
.673	.40	.156	.068	2.30
.627	.46	.185	.070	2.65
.586	.50	.213	.071	3.00
.588	.44	.220	.068	3.06
.529	.54	.237	.079	3.00
.529	.64	.331	.094	3.53
.562	.59	.339	.083	4.09
.563	.46	.222	.065	3.43
.553	.29	.073	.044	1.64
Station 4				
0.976	0.50	0.153	0.086	1.78
.961	.52	.168	.093	1.80
.922	.52	.175	.094	1.87
.869	.52	.173	.094	1.84
.787	.53	.190	.099	1.92
.705	.55	.224	.104	2.14
.656	.60	.262	.112	2.33
.618	.68	.306	.121	2.53
.581	.74	.320	.126	2.54
.531	.95	.354	.144	2.46
.524	1.20	.528	.184	2.87
.525	1.22	.640	.192	3.33
.525	1.14	.576	.171	3.38
.524	.95	.544	.128	4.25

p_d/H_0	δ	δ^*	θ	δ^*/θ
Station 5				
0.976	0.71	0.262	0.134	1.96
.963	.75	.292	.143	2.04
.922	.78	.317	.150	2.12
.862	.79	.325	.151	2.14
.783	.85	.365	.163	2.24
.715	.91	.418	.177	2.37
.662	1.00	.472	.185	2.55
.622	1.12	.535	.208	2.58
.589	1.24	.522	.219	2.39
.534	1.72	.537	.278	1.93
.532	2.13	.862	.349	2.47
.530	2.15	.936	.362	2.59
.533	2.21	.960	.361	2.66
.530	2.12	.997	.330	3.02
.534	1.96	.974	.308	3.16
Station 6				
0.926	1.14	0.636	0.151	4.21
.821	1.28	.654	.198	3.30
.748	1.54	.797	.246	3.24
.712	1.69	.758	.285	2.66
.671	1.63	.698	.280	2.50
.633	1.96	.752	.330	2.28
.593	2.83	1.035	.455	2.27
.537	2.89	1.221	.456	2.68
.516	3.50	1.630	.442	3.68
.513	3.10	1.610	.409	3.94
.514	3.00	1.590	.385	4.13
.514	2.10	1.556	.348	4.47
Station 7				
0.971	1.32	0.587	0.204	2.87
.961	1.42	.640	.262	2.44
.946	1.43	.670	.257	2.60
.921	1.40	.718	.248	2.90
.863	1.44	.669	.264	2.54
.783	1.54	.716	.278	2.57
.709	1.64	.772	.269	2.87
.640	1.71	.810	.287	2.82
.647	1.72	.876	.290	3.02
.590	1.72	.754	.287	2.62
.534	2.40	.848	.367	2.31
.530	3.26	1.366	.496	2.74
.529	3.45	1.636	.489	3.34
.533	3.92	1.596	.525	3.04
.529	3.90	1.573	.501	3.14
.530	3.86	1.452	.516	2.82
.529	3.91	1.536	.484	3.18

TABLE III.—BOUNDARY-LAYER RESULTS—Continued

(b) 12°,10-Inch Diffuser; $\delta^*_i/D_i=0.0122$

p_s/H_0	δ	δ^*	θ	δ^*/θ
Station 1				
0.975	0.63	0.109	0.090	1.21
.954	.70	.122	.099	1.23
.908	.70	.121	.097	1.24
.859	.71	.122	.101	1.21
.809	.70	.117	.097	1.20
.778	.69	.123	.098	1.26
.753	.69	.118	.098	1.21
.723	.67	.118	.098	1.21
.608	.69	.123	.101	1.22
.545	.66	.130	.100	1.30
.531	.66	.127	.097	1.31
.522	.63	.119	.097	1.23
.520	.68	.126	.096	1.32
.520	.62	.116	.093	1.25
.518	.66	.122	.096	1.27
Station 2				
0.991	0.71	0.133	0.104	1.28
.975	.71	.132	.104	1.27
.946	.75	.142	.113	1.26
.909	.76	.145	.112	1.30
.859	.75	.132	.107	1.23
.809	.75	.141	.107	1.32
.778	.73	.140	.105	1.33
.753	.75	.142	.107	1.33
.723	.75	.153	.114	1.34
.617	.71	.158	.114	1.39
.538	.71	.149	.108	1.38
.515	.69	.119	.098	1.21
.507	.63	.104	.085	1.22
.509	.64	.110	.085	1.29
.509	.63	.109	.086	1.27
.507	.63	.099	.086	1.15
Station 3				
0.989	1.03	0.286	0.180	1.59
.974	1.02	.271	.174	1.56
.944	1.05	.263	.179	1.50
.908	1.06	.276	.179	1.54
.859	1.02	.267	.173	1.54
.807	1.03	.272	.178	1.53
.782	1.03	.294	.167	1.76
.753	1.02	.292	.172	1.70
.721	1.02	.304	.171	1.78
.618	1.05	.342	.180	1.90
.538	1.03	.369	.174	2.12
.515	1.08	.417	.174	2.40
.507	1.10	.448	.162	2.77
.506	1.04	.426	.139	3.07
.509	.89	.344	.116	2.97
.507	.89	.205	.124	1.65
Station 4				
0.992	1.01	0.442	0.158	2.80
.974	1.23	.386	.226	1.71
.943	1.27	.380	.232	1.64
.910	1.25	.365	.222	1.64
.860	1.20	.361	.216	1.67
.810	1.25	.402	.229	1.76
.780	1.26	.407	.231	1.77
.755	1.26	.418	.232	1.80
.724	1.24	.412	.228	1.81
.614	1.33	.501	.241	2.08
.550	1.37	.520	.247	2.11
.517	1.44	.579	.250	2.32
.507	1.43	.636	.255	2.49
.507	1.44	.650	.239	2.72
.509	1.36	.629	.210	3.00
.509	1.26	.592	.202	2.93

p_s/H_0	δ	δ^*	θ	δ^*/θ
Station 5				
0.991	1.62	0.783	0.215	3.65
.973	1.67	.635	.314	2.02
.945	1.66	.608	.311	1.96
.910	1.63	.602	.310	1.94
.859	1.65	.603	.308	1.96
.806	1.67	.626	.314	2.00
.785	1.66	.649	.313	2.07
.740	1.66	.641	.315	2.04
.728	1.66	.647	.316	2.05
.620	1.85	.771	.345	2.23
.537	1.97	.822	.366	2.24
.512	2.04	.910	.353	2.58
.507	2.04	.905	.382	2.37
.509	2.16	.979	.386	2.54
.509	1.97	.953	.382	2.63
Station 6				
0.990	1.99	0.989	0.329	3.01
.974	2.00	.870	.385	2.26
.943	2.04	.858	.388	2.21
.910	2.00	.858	.386	2.22
.857	2.03	.885	.383	2.31
.807	2.10	.922	.400	2.31
.780	2.04	.910	.391	2.33
.750	2.11	.941	.402	2.34
.718	2.10	.960	.403	2.38
.623	2.24	1.058	.419	2.53
.544	2.36	1.089	.458	2.38
.516	2.44	1.134	.475	2.39
.507	2.56	1.191	.474	2.51
.506	2.67	1.231	.503	2.54
.509	2.65	1.293	.480	2.69
Station 7				
0.990	2.37	1.328	0.284	4.67
.974	2.56	1.280	.351	3.64
.943	2.32	1.081	.426	2.54
.908	2.40	1.109	.440	2.52
.858	2.41	1.131	.447	2.53
.807	2.40	1.142	.453	2.52
.778	2.43	1.186	.453	2.62
.755	2.43	1.196	.456	2.62
.721	2.44	1.199	.456	2.63
.620	2.62	1.328	.465	2.86
.546	2.54	1.282	.498	2.58
.518	2.66	1.380	.509	2.71
.507	2.80	1.282	.520	2.47
.509	2.88	1.461	.521	2.81
.507	2.83	1.485	.519	2.86

TABLE III.—BOUNDARY-LAYER RESULTS—Continued

(c) 12°,21-Inch Diffuser; $\delta^*_i/D_i=0.0017$

p_i/H_0	δ	δ^*	θ	δ^*/θ
Station 1				
0.991	0.14	0.027	0.021	1.31
.957	.16	.032	.026	1.23
.915	.18	.038	.032	1.21
.882	.12	.024	.019	1.28
.828	.13	.026	.021	1.22
.776	.15	.032	.024	1.36
.724	.11	.020	.015	1.33
.657	.15	.036	.026	1.40
.593	.14	.036	.029	1.24
.552	.15	.031	.023	1.37
.538	.09	.017	.014	1.21
Station 2				
0.987	0.23	0.045	0.037	1.22
.956	.42	.122	.082	1.49
.912	.32	.069	.057	1.20
.890	.34	.100	.066	1.52
.827	.33	.091	.061	1.49
.731	.35	.105	.062	1.69
.713	.35	.102	.074	1.37
.647	.39	.098	.069	1.42
.599	.40	.126	.092	1.38
.543	.58	.320	.227	1.41
.540	.59	.350	.238	1.47
Station 3				
0.987	0.74	0.180	0.128	1.41
.954	.70	.172	.115	1.49
.915	.71	.208	.138	1.51
.890	.68	.181	.119	1.52
.828	.60	.164	.104	1.58
.773	.71	.186	.131	1.42
.738	.74	.201	.131	1.54
.685	.82	.226	.154	1.47
.654	.86	.255	.167	1.53
.596	.95	.290	.184	1.58
.551	1.37	.450	.288	1.57
.530	1.88	.632	.390	1.62
Station 4				
0.983	1.42	0.328	0.221	1.42
.951	1.16	.304	.204	1.49
.910	1.27	.280	.191	1.47
.873	1.22	.328	.218	1.51
.798	1.23	.308	.212	1.45
.743	1.42	.416	.263	1.58
.694	1.47	.428	.282	1.52
.651	1.52	.446	.284	1.57
.597	1.75	.526	.335	1.57
.553	2.08	.732	.430	1.70
.530	2.12	.740	.413	1.79
Station 5				
0.980	1.82	0.386	0.292	1.32
.948	1.76	.533	.325	1.81
.898	2.09	.480	.313	1.53
.875	1.74	.430	.286	1.50
.800	1.76	.484	.308	1.57
.771	1.96	.534	.353	1.51
.691	2.56	.618	.407	1.52
.655	2.76	.584	.443	1.32
.593	2.70	.720	.504	1.43
.553	3.07	.912	.610	1.49
.537	3.36	.988	.637	1.55
Station 6				
0.987	2.85	0.823	0.511	1.61
.949	3.50	.990	.620	1.60
.912	3.23	.911	.554	1.65
.871	3.38	.888	.556	1.60
.800	3.55	1.054	.634	1.66
.765	3.20	.948	.572	1.64
.726	3.31	.981	.605	1.62
.682	3.59	1.149	.648	1.75
.658	3.87	1.312	.698	1.88
.598	4.10	1.280	.796	1.61
.554	4.80	1.593	.942	1.69
.534	5.02	1.664	.977	1.70
.528	4.80	1.538	.902	1.70

(d) 12°,21-Inch Diffuser; $\delta^*_i/D_i=0.0095$

p_i/H_0	δ	δ^*	θ	δ^*/θ
Station 1				
0.953	0.93	0.180	0.138	1.30
.916	.91	.180	.134	1.34
.886	.95	.173	.143	1.21
.826	.92	.165	.135	1.22
.800	.85	.166	.131	1.27
.738	.94	.194	.157	1.24
.684	.90	.183	.142	1.28
.540	.83	.163	.124	1.31
.539	.83	.148	.120	1.23
.530	.77	.148	.111	1.34
Station 2				
0.952	1.28	0.327	0.225	1.45
.916	1.32	.280	.215	1.30
.884	1.46	.337	.232	1.45
.820	1.35	.330	.215	1.53
.795	1.28	.328	.215	1.52
.728	1.42	.341	.222	1.53
.684	1.35	.359	.229	1.57
.550	1.47	.444	.266	1.65
.538	1.42	.438	.251	1.74
.528	1.58	.467	.267	1.75
Station 3				
0.952	2.10	0.534	0.355	1.51
.917	1.89	.508	.330	1.54
.886	1.95	.552	.364	1.52
.822	2.03	.572	.367	1.56
.793	1.96	.578	.362	1.60
.721	1.85	.590	.357	1.65
.692	2.12	.686	.398	1.73
.554	2.62	.934	.486	1.92
.536	2.25	.832	.430	1.94
.527	2.30	.870	.443	1.96
.524	2.45	.880	.436	2.02
Station 4				
0.952	2.68	0.802	0.490	1.64
.920	2.93	.908	.514	1.77
.884	2.87	.886	.522	1.70
.820	2.75	.900	.511	1.76
.801	2.87	.962	.521	1.85
.734	3.00	1.048	.554	1.89
.688	3.17	1.188	.601	1.98
.553	3.58	1.448	.678	2.14
.541	3.22	1.290	.616	2.09
.530	3.27	1.300	.631	2.06
.525	3.14	1.326	.633	2.10
Station 5				
0.952	3.55	1.130	0.651	1.74
.918	3.77	1.444	.676	2.14
.886	3.60	1.252	.701	1.79
.822	3.75	1.336	.717	1.86
.796	3.67	1.460	.698	2.09
.732	4.05	1.528	.746	2.05
.688	4.16	1.766	.798	2.21
.546	4.10	1.808	.874	2.07
.539	4.35	1.748	.833	2.10
.533	4.25	1.652	.817	2.02
.524	4.90	1.852	.919	2.02
Station 6				
0.952	4.48	1.652	0.848	1.95
.915	5.13	1.960	.946	2.07
.880	5.00	2.016	.949	2.13
.811	4.67	1.964	.914	2.15
.802	5.65	2.428	1.046	2.32
.708	5.31	2.372	1.001	2.37
.687	5.70	2.776	.932	2.98
.552	7.10	3.452	1.002	3.45
.544	5.80	2.576	1.030	2.50
.531	5.85	2.604	1.102	2.36
.529	6.00	2.604	1.044	2.49

TABLE III.—BOUNDARY-LAYER RESULTS—Concluded

(e) 23°,21-Inch Diffuser; $\delta^*_i/D_i=0.0017$

p_i/H_0	δ	δ^*	θ	δ^*/θ
Station 1				
0.949	0.19	0.038	0.030	1.28
.872	.17	.036	.030	1.20
.812	.19	.035	.028	1.24
.733	.17	.032	.025	1.27
.538	.14	.028	.021	1.34
Station 2				
0.915	0.27	0.081	0.066	1.23
.828	.34	.171	.107	1.60
.784	.41	.117	.089	1.31
.740	.49	.179	.111	1.62
.672	.55	.129	.095	1.35
.644	.60	.289	.142	2.04
.605	.60	.390	.160	2.44
.594	.58	.296	.196	1.51
Station 3				
0.958	0.75	0.336	0.201	1.67
.876	.89	.349	.210	1.66
.802	1.00	.373	.244	1.53
.745	1.12	.442	.286	1.55
.727	1.54	.481	.315	1.53
.643	1.85	.638	.377	1.69
.602	1.60	.772	.379	2.04
Station 4				
0.945	1.49	0.502	0.300	1.67
.871	1.44	.526	.346	1.52
.803	1.46	.471	.331	1.43
.741	3.15	.975	.532	1.83
.721	1.64	.544	.365	1.49
.647	3.00	1.088	.581	1.87
.604	2.94	1.320	.630	2.09
Station 5				
0.956	2.26	0.869	0.434	2.00
.881	2.62	.935	.477	1.96
.820	2.90	.940	.522	1.80
.756	1.45	.506	.344	1.47
.744	3.80	1.003	.604	1.66
.649	1.77	.648	.429	1.51
.613	2.50	.801	.511	1.56
Station 6				
0.956	3.73	1.745	0.649	2.69
.925	3.70	1.723	.551	3.13
.923	3.80	1.813	.700	2.59
.886	3.55	2.007	.739	2.72
.882	3.46	1.849	.778	2.38
.826	5.00	2.126	.848	2.51
.753	6.06	1.917	.888	2.16
.739	7.90	2.945	1.029	2.86
.647	9.20	3.156	1.328	2.38
.604	3.85	1.784	.720	2.48

(f) 23°,21-Inch Diffuser; $\delta^*_i/D_i=0.0095$

p_i/H_0	δ	δ^*	θ	δ^*/θ
Station 1				
0.951	1.06	0.200	0.164	1.22
.889	.96	.179	.147	1.23
.833	1.01	.198	.158	1.25
.777	.92	.156	.122	1.28
.720	.86	.149	.116	1.29
.632	.85	.151	.118	1.28
Station 2				
0.950	1.56	0.381	0.269	1.42
.886	1.56	.377	.272	1.38
.831	1.45	.393	.275	1.43
.768	1.43	.399	.277	1.44
.708	1.58	.432	.290	1.49
.627	1.46	.472	.292	1.61
Station 3				
0.954	2.62	0.766	0.437	1.75
.889	2.45	.783	.453	1.73
.834	2.42	.817	.438	1.87
.781	2.40	.881	.475	1.86
.708	2.44	.983	.499	1.97
.628	2.65	1.104	.457	2.41
Station 4				
0.951	4.80	1.424	0.641	2.22
.883	4.20	1.479	.609	2.43
.827	3.57	1.541	.670	2.30
.771	3.92	1.692	.609	2.78
.719	3.97	1.703	.706	2.41
.632	4.25	1.949	.616	3.17
Station 5				
0.953	5.75	2.630	0.789	3.33
.877	5.43	2.398	.789	3.04
.825	5.43	2.368	.917	2.58
.760	5.10	2.512	.823	3.05
.711	5.30	2.403	.866	2.77
.631	5.75	2.923	.874	3.34
Station 6				
0.919	7.37	3.951	0.876	4.51
.849	6.45	3.534	.925	3.82
.757	5.95	3.569	.822	4.34
.716	6.55	3.566	.885	4.03
.632	6.50	3.886	.847	4.59